

Mechanics of Dynamic and Deformable DNA Nanostructures

Ruixin Li, Anirudh S. Madhvacharyula, Yancheng Du, Harshith K. Adepu, Jong Hyun Choi*

School of Mechanical Engineering, Purdue University
585 Purdue Mall, West Lafayette, Indiana 47907, United States
Corresponding author: jchoi@purdue.edu

ABSTRACT

In DNA nanotechnology, DNA molecules are designed, engineered, and assembled into arbitrary-shaped architectures with predesigned functions. Static DNA assemblies often have delicate designs with structural rigidity to overcome thermal fluctuations, whose design strategies have been studied extensively. Dynamic structures reconfigure in response to external cues. Such transformational mechanisms have been explored to create dynamic nanodevices for environmental sensing, payload delivery, and other applications. However, the precise control of reconfigurable dynamics has been a challenge due partly to flexible single-stranded DNA connections between moving parts. Deformable structures are special dynamic constructs with deformation on double-stranded parts and single-stranded hinges during reconfiguration. These structures often have better controls in programmed deformation. However, related deformability and mechanics, as well as deformation mechanisms are not well understood or documented. In this review, we summarize the development of dynamic and deformable nanostructures from the mechanics perspectives. We present deformation mechanisms such as single-stranded DNA hinges with lock-and-release pairs, jack edges, helicity modulation, and external loading. Theoretical and computational models are discussed for understanding the deformations and mechanics, including commonly used elasticity theory, finite element method, and coarse-grained molecular dynamics models. Other special models are also introduced. We elucidate the pros and cons of each model and recommend design processes based on the models. The design guidelines should be useful for those who have limited knowledge in mechanics as well as expert DNA designers. After presenting unique applications, we conclude with current challenges in dynamic and deformable structures and outlook for the development of the field.

KEYWORDS

DNA self-assembly, DNA nanostructures, mechanics, mechanical deformation, structural properties

1 INTRODUCTION

DNA usually functions under the central dogma of molecular biology.¹ That is, DNA molecules are transcribed into RNA which is then translated into peptides, proteins, and enzymes. The genomic information carried by DNA can guide them to assemble into intricate structures and perform programmed functions in cells, including intracellular trafficking, apoptosis, migration, division, etc. The shapes and structures of biomolecular assemblies are critical in their functions. Thus, the understanding of their geometries and related mechanics is the key in structural biology. In DNA nanotechnology, DNA molecules are engineered to directly assemble into complex architectures and perform similar mechanisms and functions. This is based on the Watson-Crick base-pairing principles, where A hybridizes with T and G binds with C, which may be used as a programmable bottom-up manufacturing strategy. This idea was first proposed in 1982 by Seeman who designed a four-way junction from several DNA strands.² Since then, numerous structures and complex geometries have been explored. Initially, DNA structures were not well-defined nor rigid. A following milestone was the double-crossover motif.³⁻⁵ With the sticky-end association,⁶⁻⁸ 1D and 2D assemblies were made possible with a reasonable stiffness. However, this type of assembly did not guarantee the structural addressability which is critical in programming functions. This method later developed into the DNA tile approach, which uses a few strands to form a unit (motif) and then associate the units via sticky ends. Recently, a similar yet distinct method called DNA bricks was introduced where a large number of unique oligonucleotides assemble into desired conformations with each behaving like a brick (analogous to Lego bricks).⁹ Both DNA tile and brick methods produced complex architectures with various functions. The DNA bricks have shown excellent addressability.

A DNA origami approach pursues a different direction. This approach uses a long single-stranded DNA (ssDNA) as a scaffold in conjunction with multiple oligonucleotides (termed staples) to secure the scaffold into desired shapes. This concept was first introduced with a macromolecular octahedron made of a 1669-nucleotide (nt) long scaffold and five 40-nt staples.¹⁰ Later, Rothemund demonstrated several distinct structures in the well-recognized DNA origami work using 7249-nt M13mp18 phage DNA as a scaffold.¹¹ With the same scaffold, various geometries can be created with different sets of staples. DNA origami has been extremely popular because arbitrary shapes can be constructed in one-step annealing and the process is reliable, robust, and fault-tolerant.¹²⁻¹⁴ The size of a single DNA origami structure is limited by the length of the scaffold. However, larger structures are possible by employing multiple orthogonal scaffold strands or by linking multiple preformed DNA origami with linkers (special staples that combines segments of different scaffolds).¹⁵⁻¹⁸

In addition to the development of various static constructs, dynamic and deformable structures have also been explored for resembling protein-based dynamic motors and reconfigurable assemblies. Commonly available structures with dynamics and reconfigurability are DNA walkers,¹⁹⁻²⁵ molecular beacons,²⁶⁻²⁹ and switches.³⁰⁻³⁴ These dynamic DNA assemblies are typically made of one or few strands forming a motif without rigid domains and dependable connections. They are small (usually, about 10 nm or less) and rely mostly on soft ssDNA segments. Therefore, structural deformations, that is, shape changes of rigid dsDNA parts, are missing. These all-flexible complexes are not considered in this review. Rather, this article will include another type of well-established dynamic and deformable structures which usually have two (or more) rigid parts linked with a soft connection. The reconfiguration is often realized by a 'locking'

mechanism which forms a solid dsDNA connection between the two rigid parts. The locking mechanism may be released by strand displacement, enzymatic reactions, or molecular recognition events. Most of such structures switch between two distinct conformations, such as open and closed states. Thus, precise shape control may not be straightforward when the connection is soft.

More precise progressive control may be realized by intercalators and other chemical adducts.³⁵⁻⁴¹ This method usually applies on dsDNA helices, thus the structures formed by several closely packed dsDNA helices will be reconfigured or deformed in response to the adducts. There are also other DNA structures which deform due to external loading. The loading can be created by direct mechanical methods or by electric or magnetic fields. The dynamic mechanisms and deformable structures are the major focus of this review. Large and complex as well as dynamic and deformable architectures have been increasingly more desired and as such pursued heavily. Given the minimum structural resolution of a single base-pair, size and complexity increase simultaneously. Dynamic motions and structural deformations also add to the complexity. Therefore, the importance of relevant mechanics has elevated. Besides, we find that although dynamic systems have been explored, those with actuation or deformation on the rigid dsDNA are neither abundant nor well-modelled. The dynamic and deformable DNA nanostructures thus call for comprehensive mechanical models for better understanding and precise predictions on the structural behaviors and an explanation for the experimental observation.

We envision that the improved understanding of dynamics and deformability will benefit the designs of static structures as well. Structures often suffer from internal stresses, and thus, they may deviate from the designed conformations.^{16,42,43} For example, DNA tiles can be programmed to propagate indefinitely along the designed directions with sticky ends. However, they have limited sizes and often cyclize, forming unwanted aggregates.⁴⁴⁻⁴⁶ This is largely due to the accumulation of the stresses which may not be so serious in small structures. In addition, DNA assemblies are also subjected to thermal fluctuations. The synthesized DNA structures may resemble the design, but their conformations may have a distribution. Sometimes the variation can be non-negligible. Both internal stresses and thermal fluctuations require rational designs based on the mechanics such that the structure can be compliant (*i.e.*, the parts work together without creating stresses at the boundaries between them) and stiff enough against small variations.

In this review, we present detailed discussion on mechanics of dynamic and deformable DNA nanostructures. Our major focus is the dynamic structures with a reasonable size and geometrical complexity, which undergo structural transformation and deformation by various methods. We first introduce the basic knowledge in mechanics relevant to the DNA nanotechnology. Then we explain the mechanics of static structures so that the development of deformable DNA structures is depicted. We also discuss deformable structures by introducing different types of deformation methods based on mechanics. We provide insights on the mechanics along with models in design principles of deformable structures. Several synthesis and characterization methods are also included. Finally, we discuss representative applications of dynamic and deformable DNA structures as well as current challenges and outlook.

2 FUNDAMENTALS OF STRUCTURAL MECHANICS

DNA is particularly suitable for creating complex structures because of their excellent programmability and structural predictability.⁴⁷ Two complementary single strands form a double

helical rod with ~ 2 nm in diameter and ~ 3.5 nm in height in a full turn (~ 10.5 base-pairs or bp per turn) under natural conditions. The double-stranded (ds) DNA strands can be programmed to assemble into desired geometries. A sound understanding of the theory of elastic beams and kinematic mechanisms will allow us to incorporate these structures with the ability to perform complex maneuvers. Previous studies have used DNA as a building block to create nanoscale mechanisms.⁴⁸ This chapter introduces the basic concepts involved in designing mechanisms and the foundations of the elasticity theory.

A kinematic mechanism is comprised of linkages (or edges) and joints. A link is a rigid body that has at least two nodes, *i.e.*, points of connection to other linkages. Based on the number of nodes, a linkage is classified as a binary, ternary, and quaternary link having two, three, and four nodes, respectively. A joint is a connection between two links that allows some degree of motion. Linkages and joints together form kinematic chains. A kinematic chain in which at least one of the links is grounded or attached to the frame of reference is called a mechanism.⁴⁹ The motion of a mechanism is described with respect to a frame of reference, *i.e.*, a set of axes used to describe the position of each object. An essential idea in the design of mechanisms is the degrees of freedom (DOF) of a mechanism, that is, the number of independent parameters needed to completely describe the position at any point of time. For instance, a rigid body on a plane has three DOF, namely, x , y , and θ , as shown in Figure 1(a). For a rigid body in 3D space, it possesses 6 DOF which are the three positional coordinates, x , y , and z as well as three angular coordinates, θ , ϕ , and ψ . With all these, its possible motions can be described completely.

The DOF of a system are determined by the number of linkages and joints and the types of joints in a system. There are several kinds of joints based on the number of DOF they allow and the type of contact between them. Joints with point contact are termed lower pair joints, while those with surface or line contact are called higher pair joints. A rotating pin joint and a slider joint both offer 1 DOF. A pin-in slot joint and cylindrical joint both have 2 DOF each, while a spherical joint possesses 3 DOF. In DNA nanostructures, a pin joint can be as simple as a short strand of unpaired nucleotides connecting two DNA helical linkages. A few examples of the different types of joints, namely, revolute joint, slider joint, and slider crank mechanism, are depicted in Figure 1(b).

The concept of DOF is invaluable during the design of nanostructures to decide the range of motions we want to incorporate. It is important to note that a planar mechanism has only one ground link, even if multiple links in the mechanism are grounded. This is because the system has one ground plane. A systematic way to calculate the number of DOF of a planar mechanism is using the Kutzbach equation (Eq. 2.1):

$$DOF = 3(L - 1) - 2(J_1) - J_2 \quad (2.1)$$

where L is the total number of links. J_1 and J_2 are the numbers of lower pair and higher pair joints respectively. Using this, we can calculate the degrees of freedom of the mechanisms in Figure 1(b) to be 1 DOF each. A visualization of a DNA nanostructure as a system of links and joints is shown in Figure 1(c)-(e). Some common mechanisms are the slider-crank mechanism,⁵⁰ the crank-rocker mechanism,⁵¹ and quick return mechanisms.⁵²

An inherent assumption of the theory of mechanisms is that the links in the mechanism are rigid members. However, the behavior of DNA nanostructures which exhibit some degree of flexibility can be understood by the engineering theory of elasticity. DNA and other polymeric structures

have also been analyzed by more complicated models such as the worm-like chain (WLC) model,⁵³ which will be discussed in the later part of this article. Previous studies have provided concrete examples that show the utility of the elastic beam theory in understanding phenomena such as the folding kinetics of DNA origami tiles.⁵⁴ It is also useful when the nanostructures synthesized have curved edges rather than straight rods.⁴² A beam, in an engineering sense, is a member used to support and transmit forces. The elastic beam theory primarily focuses on prismatic beams with high aspect ratios (length/diameter), *i.e.*, having a uniform cross-section throughout their length. This assumption holds true for most DNA nanostructures as they are made up of members with uniform cross-sections. The first step in studying elasticity is the concept of stress and strain.

The stress experienced by the member is defined as the force per unit area. An elastic member can experience both axial and shear stress caused by longitudinal and transverse forces, respectively. A pair of distanced, equal magnitude forces acting in opposite directions generate a moment (M) or torque. Beams experience bending when moments act perpendicular to the axis. Torsion is caused by moments around the axis. To quantify deformation, strain is defined as the deformation of a member per unit length. Similar to stress, it can be classified into axial strain when perpendicular to the surface and shear strain when parallel to it. In general, indicial notation is used to denote the stress and strain experienced by the body. The various forces that a rod can be subjected to, and the quantitative definitions of corresponding stress and strain are shown in Figure 2(a)-(c).

The foundation of analyzing the deformation of a body and its relation to stress and strain is Hooke's law. The Hooke's law states that the resultant strain in a body is directly proportional to the stress applied. The constant of proportionality relating these two parameters is the Young's modulus (E). In general, the Young's modulus is obtained by calculating the slope of the stress-strain curve in the elastic region. Several previous studies have worked towards determining Young's modulus of the DNA helix, which was found to be on the order of 100 MPa.⁵⁵ An elastic member, in general, can undergo axial compression/tension, twist or torsion, and bending. Analogous to the Young's modulus for axial forces, the shear modulus (G) is defined for torsion. The flexibility and shape of DNA nanostructures can now be predicted through finite element method (FEM) analysis and molecular dynamics (MD) simulations on platforms such as CanDo⁵⁶ and oxDNA⁵⁷. It should be noted that the mechanical properties of these structures vary significantly depending on the surrounding environment. Thus, the medium where they are present should also be accounted for while considering their structural moduli.⁵⁸ These devices also exhibit interesting behaviors when subjected to forces. The forces applied may lead to the separation of hydrogen bonds between base-paired nucleotides, thus altering the properties of the structure further. Additionally, the elastic constants are also affected by nicks in the DNA helix, which have been found to reduce the stiffness by a factor of 100.⁵⁹ The elastic parameters help us correlate the mechanical and thermodynamic behaviors of these systems by estimating the strain energy stored in the structure and relating them to the free energy change generated due to strand displacements. The strain energy of an elastic rod is defined in Eq. 2.2.^{58,60}

$$U = \int \sigma \cdot \varepsilon dv \quad (2.2)$$

In the above equation the strain energy per unit volume v is U and can be obtained by integrating the product of stress σ and strain ε . This is analogous to the basic definition of work $W = F \times s$ as a product of force and displacement. Apart from the energy stored, it is also useful to understand

the response of a beam to external force. A comprehensive yet concise representation of this behavior of the material is provided by its σ - ε curve. The σ - ε plot of a general material is provided in Figure 2(d). The initial portion of the curve is reversible elastic deformation with constant Young's modulus which can be summarized by the Hooke's law. Beyond the linear range, the behavior transitions into irreversible plastic deformation followed by fracture at higher stress. For comparison the force extension plots of dsDNA and ssDNA are also provided (Figure 2(e)). Because of the involvement of more complex factors such as strand dissociation, the behaviors are not equivalent. However, it is evident that dsDNA and ssDNA have different regimes of nearly constant Young's modulus (Figure 2(e)). Thus, the behavior in these regimes can be accurately predicted using simple equations directly relating the stress and strain, and thus renders the elasticity theory relevant in this context.

While Hooke's law successfully characterizes the elastic regime, beams may also undergo irreversible deformation when subject to sufficiently high forces. This is known as plastic loading. When beams are unloaded after plastic loading, they experience permanent, irreversible deformation known as residual strain. A comparison of loading-unloading curves for elastic and plastic loading is depicted in Figure 2(f)-(g). It can be observed that once the stress has passed the yield strength, *i.e.*, the point which the behavior shifts from the elastic to plastic regime, the material experiences residual strain. Upon reloading, the force extension curve experiences a horizontal shift, starting from the x -intercept of the unloading curve, rather than the origin.

3 STATIC DNA STRUCTURES

Over the past four decades, DNA nanotechnology has produced complex 1D, 2D and 3D structures with various geometries. In the early years, the assembled structures were predominantly static. These structures vary in size from small constructs (*e.g.*, few-strand motifs) to macroscopic crystals. While DNA self-assembly may propagate indefinitely in theory, there is a size limit in practice due to the material availability, inherent curvature, and internal stresses.⁶¹ Well-defined DNA assemblies can be up to approximately 500 μm in size.⁶²

The simplest 1D structures are DNA rods which usually have a few dsDNA with some double crossover connections to hold them together.⁶³ The rods may be constructed with various cross-sections. For example, 6 dsDNA bundles may form a rod with a cross-section of 3 \times 2 rectangle or hexagonal arrangements. The respective square and honeycomb arrangements (or lattices) will have an impact on the placement of crossovers, resulting in some differences in DNA helicity (*vide infra*).⁶⁴⁻⁶⁶ In addition, there is a correlation between the length of a rod and its cross-sectional area. That is, the thickness of the cross-section must be at least a certain percentage of the length to avoid any significant structural deflection. This will be discussed in detail below in Chapter 5 Design Requirements and Guidelines. The rods (or linkages in the mechanics point of view) can be connected by ssDNA joints at the terminals and become wireframe structures.⁶⁷⁻⁶⁹ The wireframes may be extended into 2D or 3D structures with the joints as the corners.⁷⁰⁻⁷² In such cases, there are some hollow area in the wireframe structures. Given the same material, wireframe structures can be larger than the solid-piece structures without any cavities.

In a wireframe design, one must determine how to build the ssDNA joints. The terminals of the rods may not be on the same plane due to the nature of DNA double helix. Yan *et al.* used integer numbers of full turns on dsDNA aiming for the same plane with angles controlled by the number

of un-hybridized nucleotides at the joints (Figure 3(a)).⁶⁸ Given the integer number, the edge length may only be certain values (*e.g.*, approximately 3.5, 7, and 10.5 nm, etc.). This limits the possible configurations of wireframe structures. Bathe group further developed this approach for general design principles.⁷³ In their design, there is no need to be on the same plane. The free ssDNA segments at corners are used to form an angle as well as to compensate the plane disagreements. Versatile shapes are all available with some trade-off on the flatness. The structures may not stay perfectly in the same plane; however, the out-of-plane angle can be $\sim 10^\circ$, which is not severe and generally acceptable.

Other 1D structures can be seen as 2D or 3D designs. For example, DNA tubules or cylinders are similar to DNA rods, but their diameters may be tens of nm with hollow centers.^{15,74,75} Therefore, they can be viewed as 2D DNA sheets connected into cylinders. Another example is a DNA gear.⁶² It is similar to DNA tubules but has a diameter of ~ 450 nm. Not only can it be viewed as folded sheet, but it also has a variation along the height of the cylindrical direction. Therefore, it can either be a 2D or 3D structure. These complex 1D structures are discussed with 2D and 3D structures.

In 2D structures, a variety of geometries are possible by strand arrangements. If all the dsDNA bundles are closely packed, the structure will be a solid piece type. Due to the close packing, slight mismatch of the length and angle in a structure can accumulate. For example, flat rectangular DNA origami is usually designed with a square lattice in cadnano⁷⁶ or similar DNA CAD platforms. In the software, the helicity is often set as 10.67 bp/turn for simplicity of making crossovers (*e.g.*, 32 bp for 3 turns). However, this is different from the intrinsic helicity of B-form DNA, which is ~ 10.5 bp/turn.^{42,62} The reason is that a possible placement of a crossover is 1 every $3/2$ turns or 10.5 bp/turn yields 15.75 bp per crossover. The closest integer is 16 bp. This slight difference in helicity will cause strain throughout the assembled structure, resulting in a global curvature or twist. This effect may not show up in a structure less than 100 nm, given the limited resolutions in measurements (*e.g.*, atomic force microscopy or AFM). However, the strain can accumulate and cause significant distortion in larger structures. For example, polymerized DNA origami tiles show apparent structural twists (Figure 3(b)), while each tile does not show significant distortion.¹⁶ One way to mitigate this is adding ssDNA spacers, however, the trade-off is that the structural integrity may be compromised.

Another method is using 10.5 bp/turn for DNA helicity in the design, which is realized in honeycomb lattices. In this lattice, a crossover is placed every $2/3$ turn, which is exactly 7 bp per crossover. Therefore, there is no intrinsic mismatch and no global curvature in the assembled structures.¹⁸ Due the different crossover density, a flat plane from honeycomb lattices is thicker than one dsDNA helix. This is because the planar geometry is realized by wave-like cross-sections, as shown in Figure 3(c). In other words, honeycomb lattices realize no curvature by sacrificing the thin flat surfaces. Similar 'thick plane' effects are also available in 1D and 3D structures, but more significant in 2D structures given the characterization methods, especially AFM (see chapter 4.2).

3D structures are more complex to design and assemble. Due to the limitation of the scaffold in DNA origami, for example, 3D solid-piece structures are usually smaller than 40 nm. Small unit origami structures can be assembled together for larger assemblies; *e.g.*, gear shaped rings.⁶² This takes a significant amount of material, and the yield would suffer. Wireframe structures could be large given the cavities that are not occupied by DNA strands. Therefore, it is possible to use less

material to reach the same overall size. Since wireframe structures are not fully filled, however, the edges tend to deflect if the length is too long. The threshold is related to persistence length L_P , which is the ratio between the bending modulus κ and the environmental thermal energy $k_B T$. (k_B is the Boltzmann constant and T is the temperature).^{55,77}

$$L_P = \frac{\kappa}{k_B T} \quad (3.1)$$

At room temperature, L_P is approximately between 50 and 60 nm. This means that a single dsDNA rod will show significant bending due to the environmental thermal fluctuation if it is longer than 50 nm. To be on the safe side, the threshold may be set at 30 nm. Thus, a general rule of thumb is that below 30 nm, the assumption of individual dsDNA strands as rigid cylinders and ssDNA as soft spacers holds true. There are ways to make single edges long and straight, while sacrificing the overall scale by using more bases on each edge (Figure 4(a)).⁷⁸ One should always consider a balance between how large a structure is built with given material and how stiff the structure is.

The tile-based assemblies are normally not limited in size and can easily build into 3D structures similar to wireframe DNA origami.⁷⁹ The difference is that the starting point is an n-way joint motif with defined angle and edge number. Then the motifs are associated with each other by sticky ends and form desired structures, such as polyhedra. For example, the 3-point-star motif in Figure 4(b) provides threefold rotational symmetry and their flexibility allows them to bend and assemble into 3D tetrahedron, dodecahedron, or buckyball. If the tile were to be completely planar and stiff, they would form a large-area 2D flat crystal.⁸⁰ To make each edge of the tile flexible, the motif must be thin enough as illustrated in Figure 4(b). Since all the motifs assemble without any scaffold DNA strands, there is no trade-off between the scale and the stiffness. The limit factor would be the assembly process. The larger and more complex the final structure is, the lower the yield will be.

The DNA bricks method can generate customized 3D structures. There are two ways for the structure-building process, by either addition or subtraction. In the additive approach, the structure starts from a single strand, and neighboring strands hybridize with the first strand and propagate to occupy the space towards the target structure. In contrast, the subtractive method initiates from the entire brick with all the possible strands (which can be a cube or a rod). Similar to machining, strands related to the parts to be removed are taken away so that the target structure emerges from the rest of the strands. For example, this method can turn a brick into a toy bear,⁸¹ as shown in Figure 4(c). The stiffness is generally not a problem given the support from the base of the brick. The resolution of the assembled structures is the size of the single strands. Therefore, a trade-off between resolution and yield exists. If the strands are too short, the resolution benefits but the assembly yield may be low. The yield is usually not as high as DNA origami even with typical 32-nt-length strands, indicating that a portion of the strands are wasted. Since all the strands are unique in this approach, the cost may be significant.

There are infinite types of 2D and 3D structures. In 2D scenarios, there is a balance between flatness, curvature, stiffness, and thickness. With curvature, the assembly will either stop growing at some point or cyclize into a tube. The infinite assembly in 3D may lead to macroscopic crystals. Thus, they are also called DNA crystals. The idea was proposed by Seeman, Mao, and their coworkers.⁸² They aimed to make microscopic structures visible via self-assembly using sticky ends. Thus, this is one of tile-based structures. A tensegrity triangle was developed as an assembly unit. Via association in all three directions, 3D crystals can be built into hundreds of micrometers

in size (Figure 4(d)). There are other types of motifs developed by Yan and other groups with 4- to 6-arm motifs.^{83,84} The angle and length can be well controlled with a huge number of units coherently linking together and facing the same orientation. After the tiles are assembled, the sticky ends can be connected together by covalent bonds by ligation enzymes.⁸⁵ The crystal before and after ligation are referred as native and ligated crystals, respectively. The ligated crystals show significantly improved stability and mechanical properties. For example, they can withstand or resist external loads such as indentation far better than native crystals. They can also survive in ion-free environments. They may collapse or severely deform after drying out completely. However, they can restore their conformation when rehydrated. Therefore, their deformation behaviors and structural mechanics are of great interest.

4 DYNAMIC AND DEFORMABLE STRUCTURES

In addition to static structures with complex geometries and structural integrity, dynamic DNA materials have been explored in pursuit of building DNA nanomachines. These nanomachines benefit from the biocompatibility and programmability of DNA-based designs. Dynamic motions and reconfigurations can originate from DNA-DNA hybridization, enzyme activities, chemical stimuli, and external loadings. Here we provide a mechanical perspective on the dynamic and deformable structures along with discussions on the reconfiguration methods and tools for studying them.

The simplest and most straightforward method for dynamically reconfiguring DNA structures is by reversible assembly of units. For example, DNA origami tubules may be stacked together into a long, hollow cylinder by incorporating a set of linker strands. By removing the linkers via toehold-mediated strand displacement, the stacked cylinder may be disassembled. It may be reassembled by reintroducing linkers.¹⁵ Chen et al. used this strategy for reconfigurable chirality of a long DNA origami cylinder using multiple sets of linkers and releasers.¹⁵ Here, the involvement of rigid dsDNA parts in the reconfiguration is minimal, and there are no issues or interests from the mechanics point of view. Thus, we discuss below more interesting deformation mechanics related to structural transformation.

4.1 Reconfiguration methods

To realize nanomachines, it is essential to develop mechanisms for dynamic transformation of DNA structures and understand the related mechanics. A common strategy is altering the DOF by adding or removing restrictions from DNA-DNA binding in nanostructures.^{86,87} This can be realized by introducing signaling strands,⁸⁸ enzyme-powered reactions,^{89,90} photosensitive molecules,^{36,91} or using aptamers with target-specific affinity.⁹² Structural changes can also be performed by incorporating 'jack' strands, which alters the strain and controls the states of DNA structures. Adjusting the jack edges allows one to change the force distribution in the structures and design conformation patterns with several stages.⁹³⁻⁹⁹ Another strategy is using chemical adducts to modulate the helicity in DNA-DNA associations,³⁵ thereby changing the force states and deforming the structures progressively. Deformation of DNA nanostructures may also be induced by external loadings. External forces are applied by multiple tools including optical tweezers,¹⁰⁰⁻¹⁰² magnetic tweezers,^{63,103,104} electric fields,¹⁰⁵⁻¹⁰⁷ and AFM.¹⁰⁸⁻¹¹⁰ These devices can add forces or torques precisely and used for studying deformation mechanisms as well as mechanical properties.

ssDNA hinges with lock-and-release mechanisms

A common design for dynamic structures is involving ssDNA hinges to control the freedom of motion within their structures as well as their conformations.^{111,112} Unhybridized DNA strands are flexible and free to move around with little constraints. Addition of complementary strands will enforce structural connections and restrict the moving space of DNA by transforming ssDNA to dsDNA. From the thermodynamic viewpoint, the introduction of complementary strands creates an energetically favored state, which makes the strategy simple and applicable. One of the earliest demonstrations is the DNA tweezer (shown in Figure 5(a)) designed by Yurke and coworkers.⁸⁷ This nanodevice has two ssDNA arms sticking out in an open state initially. A closing strand hybridizes with the two arms upon introduction, resulting in the reduction of rotation freedom in the structure. The tweezer thus transforms into a closed state. This process can also be reversed with another strand that removes the constraints on the rotation of the arms. Another commonly used structure is the DNA box shown in Figure 5(b).¹¹² A ‘lock-key’ system is designed on the lid of the box. The lid is initially held tight on the box by a pair of locks which restrict the DOF. The key strands bind to the locks via strand displacement and release the double strands into a ssDNA state. This allows the lid to recover its mobility and open up. This system is similar to DNA tubules stacking together forming a long, hollow cylinder discussed above.¹⁵ However, the difference is that the lid is connected to the box via ssDNA soft spacers, thus it will close the box when the lock is presented again. In contrast, the tubules were completely disconnected and finding the same neighboring tubules during reassembly would be highly unlikely. dsDNA may also be used as rigid joints, where elastic energy can be stored and released. Ke *et al.* designed a DNA origami whose corners were locked by binding strands which were compressed as a spring.⁹⁰ Upon addition of a restriction enzyme, BamHI, the binding sites were cleaved and the compressed dsDNA were released, leading to an extended state of the structure. This type of dsDNA joints or spacers have some similarities with the jack edges (*vide infra*), but it can be seen as the joints rather than edges if they are small and the elastic energy is stored within them.

Similar controls may also be realized with environmental cues.^{113,114} For example, guanine-rich sequences often form a unique secondary conformation called G-quadruplex where four guanine bases constitute a plane in presence of K^+ or other cations.¹¹⁴ The G-quadruplex may be interrupted, thus giving back freedom of movement to sequences. I-motifs are single-stranded DNA sequences which respond to pH change.¹¹⁵ At low pH, i-motif strands fold together and reduce the DOF. At high pH, they will unfold and can perform base-pairing. Thus, they may be used for reconfiguration mechanisms for DNA structures.¹¹⁶ Other environmental conditions such as UV light has also been developed. With chemical modification, strands can be combined with photoisomerization groups or photolabile moieties; thus, upon light exposure the structures react to the environment cue and alters conformation.¹¹⁷ It should be noted that due to the nature of the DNA binding-unbinding, a precise control of multi-states is challenging with most current designs and strategies. Though some efforts have been made (*e.g.*, a three-state structure control by introducing more DNA strands to form intermediate steps),¹¹⁸ such studies are still limited and several states may coexist during the structural transitions.

Jack edges

Derived from the strategies in machine design, jack edges can provide more precise controls on structural deformation. Jack edges use a similar idea of car jacks by adjusting the length of strengthened strands (or more typically edges), and the reconfiguration can operate accordingly.

Choi group designed architected metastructures using DNA for the first time and demonstrated their auxetic reconfiguration with this strategy.⁹³ In the structure shown in Figure 5(c), adjustable jacks (in red color) are placed and can bind with different sets of strands for various lengths. With the elongation of the jacks, the structures can expand from a squeezed state to an extended conformation. By varying the jacks to desired lengths, the structure can increase or decrease its size. Note that this 2D structure, called re-entrant honeycomb, can expand in both horizontal and vertical directions simultaneously, showing negative values of Poisson's ratio (ν), a measure of relative deformation between two orthogonal directions (e.g., x and y).

$$\nu = -\frac{\Delta y/y}{\Delta x/x} = -\frac{\varepsilon_y}{\varepsilon_x} \quad (4.1)$$

where ε_x and ε_y are strain in x and y coordinates, respectively.¹¹⁹ This type of deformation behaviors is termed auxetic, thus this structure may be termed as auxetic or negative Poisson's ratio (NPR) materials. Reversible shape changes are also straightforward as current jack edges can be removed via toehold-mediated strand displacement and the sequences corresponding to the desired jacks are needed. The advantage of the jack design is that the extent of expansion can be well controlled by the length of jack edges. In their work, the intermediate states were demonstrated with several different angles and edge lengths, showing that a precise control can be achieved. Similarly, a reconfigurable DNA origami tripod with struts was reported recently.⁹⁴ The lengths of the struts can be adjusted by adding locking and releasing strands. With different lengths, the angles between the edges were adjusted accordingly; for example, angles of 30, 60 and 90°. Furthermore, the structure served as a template for gold nanorods towards plasmonic assembly.^{94,116,120-122} Another example is an origami rectangle with modular reconfiguration.⁹⁵ The origami consisted of 19×9 units and the size of each unit was controlled by an expansion strand. With replacements on different units, the structure achieved a control on the length, curvature, and twist. Overall, the length-based controls utilize the programmability of DNA designs, and this approach is capable of structural reconfiguration with high precision.⁹³⁻⁹⁹

Helicity modulation

A precise control on the helical pitch of DNA is also possible using chemical adducts. Intercalators such as ethidium bromide (EtBr) insert between base-pairs of a DNA helix, which changes the helical pitch. The intercalative binding unwinds the helicity and causes strain in the DNA structures. A recent study showed that EtBr can change the conformation of DNA origami in a progressive manner by modulating the helical pitch.¹⁶ Polymerized DNA origami tiles forms 1D ribbons as shown in Figure 5(d), where kink patterns appear periodically due to internal strain and resulting global curvature. Intercalation of EtBr changed the helicity from intrinsic 10.5 bp/turn to designed 10.67 bp/turn (square lattice). The helicity modulation compensated for the initial right-handed curvature and gradually flattens the structure, thus the kinks appeared less frequently. At 10.67 bp/turn, the micron-long origami polymers were completely planar and free of kinks. Further increase of EtBr concentration resulted in a helicity greater than 10.67 bp/turn, which overcompensated for the mismatch and led the structural transition to left-handed twists. Another study also demonstrated that adding chemical adducts can tune curved structures.³⁵ Several C-shaped monomers were put together forming a 10-bundle-crosssection left-handed spiral structure. Since dsDNA has right-handed twisting and EtBr can weaken the right-handed twist, the structure would have more left-handed twisting/curvature with the addition of EtBr. Therefore, the helical density of the spiral structure and the pitch length both decreased as the EtBr concentration increased. Another recent study demonstrated that the helicity control may be extended with photo-

modulation.³⁶ Short- and medium-wavelength ultraviolet (UV) light, UVC and UVB, can cause photo-lesion in DNA, damage the structure, and lead to the release of internal strain. As a result, curved structures may flatten. In contrast, long-wavelength UVA (315-400 nm) does not damage the DNA strands, and thus, DNA assemblies are unaffected. There are a class of photo-responsive intercalators which may be utilized to control the shape of DNA constructs in conjunction with UVA, thereby regulating their intercalative binding properties.¹²³ For example, a triarylpyridinium cation (TP1) can be biscyclized into a polycyclic form (TP2) by UVA radiation.¹²⁴ TP2 is a strong intercalator with DNA, whereas TP1 is not. Under UVA radiation, it binds with DNA like EtBr, which changes the conformation of DNA assemblies.³⁶ The photo-responsive molecule may not have sequence specificity. However, using photoactivable intercalators with UV light may provide an alternative method to sequence based designs and show possibilities of a progressive control of DNA structures remotely by external radiation.

External loading

Like any other materials, DNA nanostructures deform upon exertion of external loads. To understand the mechanics of DNA deformations, several methods have been exploited. Dietz *et al.* used an optical tweezer to study DNA linker systems.¹⁰⁰ The linkers were put between a pair of beads and extended as the beads were moved by the optical tweezer. They first tested DNA rods in honeycomb lattices with 6, 8, 10, and 12 helices and compared the force-extension between them. Then they used the 10-helix rods to test the hairpin structures with the forces to pull it open. Different hairpin designs resulted in distinct mechanical properties in folding and unfolding behaviors. Another study investigated bending and torsional rigidities of DNA bundles with magnetic tweezers.⁶³ Several DNA bundles were designed with one end fixed to a coated substrate while the other end was modified with a magnetic bead, as shown in Figure 5(e). The movement of the bead was controlled by applied magnetic forces and exerted bending as well as torsion to the structures. Several DNA structural designs were examined for their rigidities and were compared to FEM analysis. AFM can also be used for external loading studies.¹⁰⁸ A DNA crystal was constructed and nanoindentation was performed using AFM. The mechanical deformation behaviors and elastic properties were probed successfully. These studies provided useful tools and platforms to study deformation and mechanics of DNA structures. However, the precision, types of loadings, and the structural complexity that can be probed are still limited, thus more possibilities remain to be explored.

Other related methods for reinforcement

Combining DNA structures with other methods is useful for improving their mechanical and thermal properties.¹²⁵ By combining thymidines with DNA nanostructures, Dietz group showed that covalent bonds formed within the structures via UV irradiation.¹²⁶ This photo-crosslinking strengthened the designated DNA origami and improved their stability. Their results demonstrated stable structures at temperatures up to 90 °C and in pure double-distilled water, where hydrogen bond-based structures cannot remain intact. Similarly, Sugiyama and coworkers demonstrated that 8-methoxypsoralen can crosslink with pyrimidine bases in DNA origami upon photo-irradiation.¹²⁷ The crosslinked structures have improved resistance to high temperatures. Apart from photo-crosslinking, chemical crosslinking methods also have been developed.^{128,129} Shih *et al.* used polyethylene glycol (PEG) modified oligolysine-coated DNA nanostructures. With addition of glutaraldehyde, the structures can be crosslinked and show 400-fold higher resistance

to nuclease as well as improved stability in low-salt environments. The reinforced structures are also expected to have improved mechanical properties.

4.2 Experimental characterization

Given the versatility and programmability of DNA self-assembly, one can construct complex structures, which may be static or dynamic in nature. Due to their small size on the order of nanometers, it is crucial to have a proper toolbox of measurement techniques to observe or monitor the structures after synthesis. AFM, transmission electron microscopy (TEM), and fluorescence microscopy are prominent methods used for visualizing nanoscale devices.¹³⁰ While AFM and TEM are primarily used to measure structures in static states, several methods such as fluorescence microscopy and fast-scan AFM excel in monitoring real-time dynamic changes in DNA structures.

AFM has been widely used to create images with a high spatial resolution (< 5 nm) of various soft materials including DNA constructs.^{131,132} It is versatile as it can be performed in heterogeneous media like air and buffer solutions. While AFM in air involves drying the sample, imaging in buffer allows one to ensure that the measurement reflects their behaviors in native environments.¹³³ AFM was used to characterize dynamic nanodevices such as quasi-fractal patterns on a flat origami surface.¹³⁴ The states before and after dynamic process were observed by performing AFM scans of the device in 1-, 4-, and 10-cavity states, as shown in Figure 6(a). AFM has been proved to be reliable on a variety of length scales. Prior studies have successfully used AFM imaging to analyze structures ranging from a few nanometers⁶⁸ to microns¹³⁵.

While traditional AFM is generally used to image structures in their static states (or the initial and final states of dynamic structures), fast-scan AFM makes it possible to monitor the formation of 2D DNA origami lattices¹³⁶ and the assembly of DNA nanostructures on lipid bilayers.¹³⁷ The real-time movement of dynamic nanodevices such as DNA rotors¹³⁸ can be visualized with remarkable accuracy. The nanostructure is comprised of a stator and a rotor element constrained by photo-responsive oligonucleotides. The structure is imaged using high-speed AFM at a rate of 0.2 seconds per frame while being irradiated by UV light. The snapshots of the structure at various instants show the rotation of the rotor upon exposure to UV. With improving scanning speed and accuracy, high-speed AFM can also be utilized to understand the molecular dynamics of DNA nanostructures by in-situ measurements of structural changes.¹³⁹ Sugiyama and coworkers have worked towards single-molecule imaging of the enzymatic actions on DNA origami.¹⁴⁰

Apart from providing information about the topography, AFM can also be used for studying the behavior of nanostructures in response to the tip. DNA structures are flexible and can respond to variations in tip force while being imaged. The tail of dolphin-shaped DNA origami structures can be pushed to the sides by the AFM tip.¹⁴¹ More controlled force application can probe nanomechanical properties. Fundamental structural properties such as Young's modulus of DNA constructs were measured in nanoindentation experiment using AFM.^{108,109,142} During indentation, the force with respect to the separation between the AFM tip and the deepest indented point of the sample is recorded and used to calculate the Young's modulus (Figure 7(b)). The tip can also cut, fold, and stretch the surface of DNA structure.¹⁴³ Figure 7(c) shows an AFM tip cutting the rectangular and triangular DNA origami surfaces. The scans of before and after the cutting confirm the effectiveness. This may open the door for nano-manipulation. The versatility and multitude of

options that AFM offers have made it an indispensable part of any nanostructure researcher's toolbox.

Another popular technique to study DNA nanostructures is TEM. This process utilizes high-speed electron beams extracted in a vacuum for imaging. It involves the 3D reconstruction of a nanostructure using several 2D electron micrographs. This results in a highly accurate representation of the nanostructure capable of ~ 0.1 nm resolution. Imaging is usually performed using thin slices adorned with DNA structures. The samples are often stained with heavy metal ions (*e.g.*, uranyl) to improve electron scattering. The staining is either on the object of interest or by its surroundings. Staining the DNA structures is termed positive staining, which makes the DNA structures appear dark, while the other method results in bright structures and is called negative staining. Cryo-EM is used for exceptionally high resolution and measuring samples in the pristine state without staining. In this method, the sample is quickly frozen with liquid nitrogen and measured at very low temperatures (*e.g.*, -170 °C). Cryo-EM has been leveraged to capture high-resolution images of molecular structures¹⁴⁴ and verify the structural fidelity of automated DNA designs.¹⁴⁵ TEM imaging is often suited for observing static structures because the 3D reconstruction obtained is a cumulative average of several structures. Similar to AFM, TEM can observe the initial and final states of dynamic structures. Due to the vacuum environment, the sample is protected from external contamination. This method is handy for obtaining the probability distribution of the various conformations of the designed structure from which the free energy landscape of the object can be mapped. Figure 6(b) shows the TEM images used to determine the conformations of a nanostructure with an ssDNA hinge.¹⁴⁶ The snapshots of the device in various conformations allow one to map the energy profiles of the structure, thus enabling the ability to fine tune its properties as desired.

AFM and TEM have both found extensive applications in DNA nanotechnology. However, each method comes with its own share of pros and cons. While AFM is relatively fast and offers good spatial resolution, its utility is limited to 1D and 2D samples. Given the nature of the AFM probe method, precise 3D imaging is difficult. It is also hindered by the fact that the properties of the imaged structures might be different from those exhibited freely in solution. This is due to the deposition of samples on mica which leads to the flattening of the structure. Drying the sample for in air imaging will likely deform the structure and change its conformation. Cryo-EM, on the other hand, offers exceptional resolution and 3D reconstruction but requires rigorous preparation, vacuum environment, and additional postprocessing of the 2D micrographs.

Besides AFM and TEM, researchers also make use of other methods to gain insights into the behaviors of dynamic and deformable DNA structures. These include methods like Förster resonance energy transfer (FRET) that take advantage of fluorescent markers incorporated into the designed structure. Several groups have exploited FRET for observing a variety of dynamic DNA processes ranging from DNA cargo sorting robots to transformable 3D DNA structures.^{96,147,148} FRET is a distance-based energy transfer mechanism between a pair of dye molecules.¹⁴⁹ The resonance occurs because of the interactions between a fluorophore (donor) and a quencher (acceptor) when they are in close proximity. This phenomenon is marked by a decrease in observed fluorescence signal of the donor due to the overlap of the emission wavelength of the donor and the absorption wavelength of the acceptor. Due to its inverse-sixth power dependence, it has found several applications as a molecular ruler to perform distance measurement. It is particularly

invaluable while observing dynamic processes and mechanisms such as toehold-mediated strand displacement.⁹⁶ In DNA structures, FRET is introduced by strategically decorating DNA strands with fluorophore and quencher labels. An example of this method in practice is shown in Figure 6(c), which is a simple DNA machine decorated with fluorophores.⁹⁶ Whenever strand displacement occurs, the reconfigurable edge shortens in length, making the fluorophores come in close proximity and leading to a change in fluorescence. Common FRET pairs used in DNA studies include cyanine-3 and cyanine-5 (Cy3-Cy5) as well as fluorescein amidites and 5-(and-6)-carboxytetramethylrhodamine group (FAM-TAMRA). FRET measurements are pivotal in 2D and 3D cases involving biological entities (*e.g.*, cells) as they help observe phenomena occurring inside the entities where methods such as AFM and TEM become redundant.¹⁵⁰ One limit is that the fluorophore-quencher pair must be within the range for FRET to occur. This can bring challenges for the placement of the pair on the structure of interest.

In addition to visualizing a pair of points by fluorescence, DNA nanotechnology has also enabled the development of super-resolution microscopy techniques like DNA points accumulation for imaging in nanoscale topography (DNA-PAINT).¹⁵¹⁻¹⁵³ Unlike commonly used fluorescence methods, DNA-PAINT utilizes freely diffusing dyes to localize molecules. The design consists of imager (strands freely diffusing with a dye) and docking strands (affixed to the assembled DNA structures at the location of interest). The camera cannot detect the imager strands in free solution since they diffuse over several pixels within a second. However, they are fixed to a specific location for an extended period when they bind with the complimentary docking strands, allowing them to be detected. The advantage of using DNA strands is that it provides precise control over the kinetics of binding and unbinding of imager and docking strands by strategically modifying their binding affinity or the salinity of the imaging buffer.¹⁵⁴ The programmability of the binding duration helps improve the localization precision of this approach. This method has been successfully implemented in characterizing the assembly of 3D polyhedra.¹⁵⁵

There are several techniques that can provide an avenue to study mechanical behaviors. Force application through optical traps is achieved by attaching DNA handles to micrometer-sized dielectric optical beads. The force is generated due to the change in momentum of refracted photons that are shone using a laser. It must be ensured that the DNA handles are sufficiently long so that the DNA structure is far from the optical beads and is therefore protected from heating effects.¹⁵⁶ A pictorial representation of DNA nanostructures being manipulated by optical traps is shown in Figure 7(a). This method has proved useful in measuring fundamental properties of DNA like stretch modulus.¹⁵⁷ In an analogy, this method acts as a microscale device of the tension test performed for macroscopic specimens. A similar but simpler approach leverages magnetic traps to subject nanostructures to forces. The application of magnetic traps to external loading has been briefly discussed in chapter 4.1. This method is advantageous as it allows the application of a constant force without a complex feedback loop. Earlier studies have used DNA rotors attached with magnetic beads, to impart rotational motion through the application of magnetic fields. Though attaching magnetic beads to DNA devices increase complexity, it offers a reliable way for controlling nanoscale devices.

Like magnetic fields, electric fields can be leveraged for incorporating mobility into nanostructures. This approach is based on the fact that the DNA backbone is negatively charged. Consequently, these structures respond when subject to an external voltage. Earlier studies proved electric fields

as a reliable way to achieve precisely controlled motion in nanoscale mechanisms similar to DNA rotors.¹⁰⁶ Electric fields have also been able to estimate the mechanical properties of DNA helices.^{158,159} The force actuation with electric and magnetic fields may be differentiated by the fact that electric fields subject the whole structure to forces, while magnetic fields allow application of forces on specific components of the nanostructure.

4.3 Theoretical and computational models

There are several models for dynamic and deformable nanostructures. This chapter provides an overview of the models as well as the pros and cons of each model. The models are sorted based on the scale, from macroscale (continuum) to mesoscale (covering microscale to macroscale) and ultimately to microscale (atomic or molecular level). Deformable nanostructures were initially developed from macroscopic mechanical systems. Therefore, DNA structures may use similar continuum models. These include elastic beam theory and FEM for numerical simulations. Given the sub-nanometer resolution of DNA assemblies, mesoscale models may also be applied. An effective mesoscale model on polymers is the freely-jointed chain (FJC) model (or ideal chain model) among others. At the microscale, atomic or molecular models consider the interactions between particles (*e.g.*, atoms), and thus, provide significantly more detailed information. Given the enormous number of particles in the calculation domain, these models are used for simulations only. One important note here is that the models discussed in this chapter are design driven, which means that they must benefit the design process, either by revealing the mechanical properties or ensuring the deformation schemes. Practicality (*i.e.*, reasonable size or the number of particles to be calculated) is also important. Therefore, full-fledged quantum mechanics models are not considered.

Spring network models are the simplest form of elasticity theory. It can be rough or fine, depending on the size of the parts represented by the springs. Typically, a segment of continuous dsDNA is modeled as a spring with a given spring constant and initial length. The loading on a spring can be uniaxial, torsional, bending or their combinations. Chen *et al.* applied the spring system to a single-layer origami rectangle which has an original curvature.⁵⁴ The cyclization process of the tile using a set of linkers was modeled as a two-step process with an intermediate state: (i) flattening the initial curvature and (ii) rolling up into a tube. The deformation was assumed to be elastic and evenly distributed on the spring system analogy. Figure 8(a) illustrates a spring network of dsDNA bundles that experiences torsional and bending loads. The calculated energy for cyclization matched with the experiments and the simulations.¹⁶⁰ The advantage of the model includes the simplicity and accuracy for regular deformation. For a less than 100 nm scale structure, the manual calculation gives a superb precision at the uncertainty level of 1 %. The downsides are also obvious, nonetheless. The deformation should be small, simple, and evenly distributed without any concentrated spots. In their work, the deformation between the neighboring dsDNA helices was around 10°, which may be considered as small deformation. Therefore, the spring constants may be assumed as constant, not varying with any parameters or under different environmental conditions. Moreover, the deformation process must be assumed in a certain way that it can be calculated. Complex deformations may not be possible in the spring model.

The key difference between the spring system and general elastic beam theory is that the springs in the spring model have no volume and are linked with other springs only at the terminals, whereas the beams in the elasticity theory have volume and can connect with others anywhere on the

surfaces. Therefore, the beams enable more boundary conditions. For example, the elasticity theory considers how one piece of material is connected to the other. Liedl *et al.* modelled the DNA rods made of 4 to 6 dsDNA bundles as elastic beams, as shown in Figure 8(b).⁶³ By considering four different types of boundary conditions between the bundles (fully disconnected in red, fully attached in blue, and two partially attached in green and yellow), they compared the elastic beam theory with the FEM simulations. They concluded that the conditions with best agreement were the two partial attachments. A downside of the simple model is that the actual torsional rigidity may be less than predicted. There could be some uncertainties in applying the elasticity theory on complex structures since it often requires additional information. For example, Choi and coworkers applied this theory on auxetic metastructures and found that it could roughly estimate their mechanical behaviors.⁹³ However, their experiments and simulations suggested that the mechanical properties of components (edges and joints) also must be considered to accurately predict the deformation behaviors and structural properties.

FEM is a numerical method that solves a set of partial differential equations for structural analysis or other applications. The finite elements refer to smaller, simpler parts subdivided from a large system. In such a way, the equations are numerically manageable. CanDo is a widely used FEM platform in DNA nanotechnology. It has a single base-pair resolution, which means that the finite elements in CanDo are each base pair. The boundary conditions are set such that the neighboring bases can slide but not separate. CanDo offers reasonable initial values for DNA mechanical properties, and users can change the values for their specific conditions. All the simulations are normally performed online and finished within a few minutes. One of the challenges in CanDo is that applying forces is complex, which requires the users to install the CanDo related software locally and to adjust the structure manually. Another challenge is the representation of ssDNA in the simulation. No matter how long the ssDNA segment is, it is recognized as a connection without length. Thus, it cannot simulate certain structures, for example, the crank slider by Castro group, where many ssDNA connections are used.¹⁶¹ Generic FEM platforms such as COMSOL, Ansys, and ABACUS may be good alternatives. These programs are capable of all kinds of direct mechanical loadings but may require heavy work to set the system up in the generic platforms to fully depict the bases of dsDNA as well as nucleotides of ssDNA. Liedl and coworkers used the COMSOL simulations and successfully described the detailed responses to bending and twisting of DNA rods (Figure 8(b)).⁶³

The FJC model may be the simplest mesoscale model to describe polymers, including DNA. It assumes the polymer as a random walk with a set step length.¹⁶² Each step stops at a monomer. This neglects any interactions between the monomers within the polymer. The polymer may thus be modelled as more likely to have curvature than in experiments. A slightly modified model is worm-like chain (WLC), which limits the angle between the neighboring monomers.¹⁶³ This model assumes that the neighboring connections are almost in the same direction. Therefore, the polymer will remain straight. Another change can be made to the step length. It can be set as extensible,¹⁶⁴ and then, the distances between the monomers are not fixed and can change upon loading. This introduces more parameters such as stiffness so that the models can fit polymer behaviors better. In DNA molecules, the monomers are usually the bases, and thus the step is the distance between bases, which is the sugar and phosphate backbone. Dietz and coworkers used extensible WLC and extensible FJC models for conventional (2 dsDNA) and stiff (>2 dsDNA) duplex bundles, respectively.¹⁰⁰ Both models agreed with the experiments, as the tested systems were simple rods.

If large complex wireframe structures are examined, however, the chain models may not be applicable. Like elastic beam theory, it also requires additional information on which chain model to apply based on the buffer conditions and crossover designs.

MD simulations provide more detailed information with significantly better resolution. This method analyzes the physical movements of particles (*e.g.*, atoms or molecules). The particles are subjected under interactions for a set duration, producing a view of the dynamic evolution of the whole system. The trajectories of the particles are determined by numerically solving Newton's equations of motion for the particles. Coarse-grained models use a pseudo-atom to represent a group of atoms. Thus, the resolution is pseudo-atom level. OxDNA is a commonly used coarse-grained MD platform in DNA nanotechnology.⁵⁷ It uses one particle to represent one nucleotide. Seven different association energies are used to consider the connection between the backbones and the base-pairing, stacking, and other relations among the bases. The platform allows external loadings to the system. As such, this model provides significantly more details than the abovementioned methods. Choi group performed coarse-grained MD simulations on cyclization of an origami tile (Figure 9(a)) and compared the results with experiments, FEM results, and elasticity theory.^{54,160} The experiments determined the conformations only before and after the cyclization, from which related energy was estimated. A simple spring network model provided results that matched with the experiments. However, details of the deformation were missing. For example, the exact deformation pathways were not revealed (Figure 9(b)). The MD simulations on the oxDNA software calculated the forces needed to induce the cyclization and provided the details of structural evolution under loads. Overall, coarse-grained MD models are powerful tools that can include non-specific binding of bases, the charge effect of salts, and the sequence specificity.⁵⁷ Some details are not included, however; for example, the DNA form (*e.g.*, B-Z transition), pH-dependent behaviors, and other molecular effects.¹⁶⁵ The best way to consider such effects would be all-atom models.

All-atom models include all the related atoms in the simulations for better accuracy. Thus, DNA, water molecules, free ions, and base-ion complexes will all be calculated. Therefore, direct simulations of non-Watson-Crick (or noncanonical) base pairings are possible, including i-motif, G-quadplex, and other possible bindings. Nanoscale molecular dynamics or NAMD is an all-atom software that can simulate DNA structures.¹⁶⁶ It can also explore the DNA association with proteins, lipids, and carbohydrates. However, there are significant issues. Firstly, all-atom computations take significantly longer than coarse-grained models, because all the atoms are considered. Secondly, simulating deformations of large DNA structures may not be realistic even if it can take up to 1 billion atoms. Acuna *et al.* simulated the position of a fluorophore on a DNA origami using NAMD.¹⁶⁷ The simulation suggested that the fluorophore bounced back and forth due to the thermal fluctuation. Stacking and unstacking of the bases were observed. Although all-atom models can capture details, the entire simulation domain is about 50 bp (~17 nm) in size. It is difficult to calculate the overall deformation of large structures. Thus, the all-atom models are recommended for small segments rather than assembled structures. For example, the detailed behaviors of function groups (*e.g.*, pH- or ion-dependent groups) may be well described.

5 DESIGN REQUIREMENTS AND GUIDELINES

Given the focus of this review on dynamic and deformable structures, this chapter provides our recommendations for designing structures with deformability during dynamic processes. Our

guidelines presented below are based on three common models: elasticity theory, FEM, and coarse-grained MD models. Suppose a complex structure is being analyzed by FEM. The coarse-grained MD computation may also be performed to gain more details in exchange of design and modelling time. However, the elastic beam theory may not give sufficient information due to the complexity, and the experiment may not agree with the design. Note that other models such as FJC and WLC models as well as all-atom models are not discussed here since they may be best suited for special cases as discussed in chapter 4.3. For example, FJC models are applicable for long DNA rods, while all-atom models are suitable for direct simulation of non-Watson-Crick base pairings in a small domain. In the following discussion on the general designs and models, the structures are classified into two groups: solid piece and wireframe.

In solid-piece DNA nanostructures, it is generally safe to assume that dsDNA strands are rigid cylinders with deformability and ssDNA are soft spacers. Most deformations occur with ssDNA parts or thin dsDNA bundles, while thick dsDNA segments will barely deform. Conceptual designs may be verified with the elastic beam theory and examined with FEM. A rational design route may be: (1) conceptual design with assumptions on rigid dsDNA and soft ssDNA; (2) intermediate design with possible changes based on elastic beam theory; (3) final design verified by FEM simulations. Between the steps, corrections should be made on the design to reflect any parts that do not fit the design criteria (*e.g.*, a curved edge should be reinforced to be straight). Given the simplicity of the solid-piece design, not many changes are expected.

Wireframe structures can be more complex. The complexity comes from both the dsDNA edges (linkages) and ssDNA joints. Depending on the expected deformation of the dynamic structures, different strategies may be used. For small deformations ($< 10\%$ of relative changes), the assumptions of dsDNA as rigid cylinders and ssDNA as soft spacers still hold true. In such a case, they can be designed like static structures. Edges should be shorter than the persistence length, and ss-segments at joints should be designed accordingly for the range of adjustable angles. Yan *et al.* summarized correlations between the ssDNA length at a joint and the angle between two adjacent edges.⁶⁸ As depicted in Figure 10(a), the length increases from 2 to 6 nt with the angle ranging from 180° to 0° . Each ss-segment length would be suitable within the small deformation. General FEM platforms such as COMSOL may be used for better simulations on the ss-segments.

For a greater extent of deformation (*e.g.*, 10-50%), the edge rigidity and joint flexibility must be considered. Choi group developed a set of design requirements on DNA origami wireframes experiencing significant deformation ($> 30\%$).⁹³ They explored several auxetic structures which normally have sharp angles and relatively long edges. Two key points from the work are as follows (Figure 10(b)). (1) Edges must have a thickness greater than 10% of their length for sufficient rigidity. Otherwise, the edges will likely have curvature. (2) Joints must have a certain level of tension, quantified by a stretch level (length of a ssDNA segment at a joint divided by its fully stretched length) of 55 to 70%. For the stretch level below 55%, the joint will be loose, and as such the structural integrity will be compromised. On the other extreme, the joints with a stretch level of over 70% may experience internal stresses and likely distort (without any loading) due to the lack of sufficient deformability. If both recommendations are met, the assembled structures will have straight edges and sharp angles. Note that the joint stretch level is difficult to study with FEM simulations which also may not be able to reflect the changes of elastic properties under large deformation. Therefore, coarse-grained MD computation will be the best choice. Like any designs,

corrections are needed before finalizing the design. The changes on the lengths of ssDNA segments are usually not significant, for example, from 8 to 6 nt, due to the moderate deformation.

If a structure undergoes significant deformation ($> 50\%$ relative change) or is too large and complex to design, several iterations are required. A recommended design route is: (1) disassemble the structure into several components; (2) design each component based on the guidelines shown above; and (3) assemble the components and check for additional corrections on the design. Suppose a round table with four legs is the structure to be designed, and it is subjected under loads in the center of its upper surface. If the initial design is under a large force (*e.g.*, 1 nN) that might result in a significant deflection. In this case, the table may be conceptually disassembled into five components: a round tabletop surface and four table legs. The force distributed on each leg can be estimated (*e.g.*, 0.25 nN if four legs are symmetric). The design of the legs may be evaluated by FEM to ensure that they remain straight under the load. The table surface should be examined by coarse-grained MD simulations because of the significant deformation. Due to the possible large deformation, corrections on the thickness of the tabletop are expected. After the legs and the surface are ready for the assembly, the coarse-grained MD simulations may be performed for the assembled structure. Additional corrections on the connections between the legs and the tabletop or even the components themselves may be necessary. Eventually, the DNA table will be shaped. Castro and coworkers proposed a design flow on complex structures, which reflects the same idea of design.¹⁶⁸

Overall, the design recommendations are closely related to possible models on dynamic and deformable structures. Simple models, such as elastic beam theory, often require additional information of the structure and components. The effectiveness of the design purely based on simple models may thus be limited. As discussed in chapter 2, DNA properties can vary when subjected to large deformations. Therefore, complex deformable structures would require models that can account for variation of the properties. This type of model would be able to provide more detailed information about the structure; for example, coarse-grained MD models as opposed to FEM. The time for design would then increase exponentially with respect to structural complexity.

6 APPLICATIONS OF DYNAMIC AND DEFORMABLE STRUCTURES

6.1 Devices based on flexible ssDNA hinges

As discussed above, ssDNA is widely used as a joint connecting rigid DNA bundles. Its flexibility and low stiffness enable it to be a perfect joint which allows a greater degree of motion compared to dsDNA or other higher order duplexes. Castro group demonstrated the effectiveness of ssDNA hinges in the machine mechanisms constructed by DNA origami.¹⁶¹ They constructed the crank slider mechanism which outputs translation upon circulating the crank, from dsDNA bundles. The bundles were used as links of machine elements and ssDNA to control the motion of these links. The flexibility of ssDNA segments varied the crank angle, resulting in the translation of an outer bundle (slider) over the inner rod. Further, ssDNA was also used to change the conformations of a benet linkage. These basic mechanisms drive the challenge to create complex functions for nanomachines. A fully functional nanomachine may contain intricate mechanisms which contain two basic components when broken down; for example, the DNA rods are being pulled or rotated upon hinge. By standardizing the two, higher order mechanisms can be devised.

Multiple groups have developed various mechanisms for controlling cargo actuation. In an attempt to using DNA as a cargo delivery vehicle, Kjems and coworkers designed a DNA origami box with internal cavity.¹⁶⁹ The hollow volume of the DNA box may be used to carry molecular payloads and have the capability to open and close the lid with a set of locks and keys. This concept was demonstrated for drug delivery by Douglas *et al.* with DNA-aptamer locks which respond to an array of cues.¹⁷⁰ The cues can be platelet-derived growth factor (PDGF) or protein tyrosine kinase 7 (PTK7).^{171,172} The cargo in the box can be antibodies or anti-cancer agents. Thus, delivery vehicles leveraging the programmability of DNA can be effective in finding the target cells and releasing the drug molecules.

Liposomes or lipid vesicles are often used to mimic biological cell membranes. There is a challenge on controlling the size and shape of liposomes.¹⁷³ Lin *et al.* created a dynamic long and thin quadrangular prism or cylindrical DNA template for liposomes to grow on (Figure 11(a)).¹¹¹ The cylindrical template was polymerized from monomers which have two rings and four pillars such that the distance between the rings is well defined. The liposomes will form in the center of the rings in the presence of free ssDNA segments projected to the center of the rings. The pillars in the monomer can be removed (changed from dsDNA to ssDNA) so that the individual liposomal spheres can merge into a single long rod shape liposome. This development using DNA structures as a dynamic template can exponentially increase the functionalization of liposomes as synthetic vesicles.

6.2 Jack-enabled reconfigurability

Jack edges induce local strain to displace some parts within a structure, thereby changing the conformation.⁹³⁻⁹⁹ As discussed in chapter 4.1, jack edges prove to be more precise than flexible ssDNA hinges/locks. Li *et al.* designed jack edges as a structural transformation mechanism for a Hoberman flight ring.¹⁷⁴ A Hoberman sphere is a 3D deployable structure developed as a kids toy and can change its finite size upon external loading (*e.g.*, switching between compressed and extended states). Its 2D version is a Hoberman flight ring. They constructed a Hoberman flight ring with DNA origami which consisted of 6 deployable triangles in 2 layers, representing a trefoil knot. As shown in Figure 11(b), when the red triangles are located on top of blue triangles, the inscribed circle is at its largest (open state). It becomes smallest (closed state; a hexagon overall) when the red triangles slide farthest with respect to the blue ones. The structural transformation was made possible by changing the lengths of three jack edges implemented (*i.e.*, long jacks for the hexagon; short jacks for the triangle). All joints between the triangle edges are made of unpaired ssDNA segments, with their length depending on their rotation angles. About 50% change between the two conformations marks as an excellent deployable structure. This 2D reconfiguration mechanism could be extended in 3D and the volumetric change has the potential for payload delivery.

This type of deployable structure is distinct and different from regular reconfigurable structures. Typical structures capable of reconfiguration often have the conformation changed for distinct differences. Examples includes a box that opens the lid,¹¹² a tetrahedron which changes one of its edge lengths,⁹⁶ and a set of rings that stacks and disassembles.¹⁵ After reconfiguration, the symmetry is changed. In contrast, deployable structures preserve their global shapes during expansion and contraction.¹⁷⁵ In the case of the flight ring, the structure is centrosymmetric in both open and closed states. To keep the structural symmetry, the open or closed parts must be either at

the center (flight ring) or symmetric (with respect to the middle axle or the center point). The shell of cowpea chlorotic mottle virus (CCMV) can be considered to be deployable.^{176,177} Upon pH change, the shell deploys and the genetic molecules inside are released. A simplified view of the process is that the shell reconfigures from icosahedron to icosidodecahedron. In this process, the 20 equilateral triangle surfaces rotate, and 12 regular pentagon surfaces emerge. These pentagon surfaces are the channels for releasing genetic molecules from the cavity. Before and after the deployable reconfiguration, its centrosymmetric property remains the same.

6.3. Propagation of local deformation driven by information transfer

Structural deformation mechanisms discussed thus far need local deformation on each actuation site to induce global changes in configurations. With the increase in the size of DNA assemblies and the number of reconfiguration sites it becomes a challenge to supply proportional amounts of ssDNA to act on the sites. Ke *et al.* proposed a method that uses a single reconfiguration site to transform the entire structure.¹⁷⁸ The nanostructure contains repeating units of four dsDNA bundles in rhombus shapes. The structure has two stable states, corresponding to the standing and falling of the dominoes. When a trigger strand is presented, the unit that recognizes the trigger changes its configuration from standing to falling, causing all other units to fall. This work proves that the transfer of structural deformation between molecular units is possible and can be dynamically propagated with external activation. If the structure can be made longer, the sensing (of ssDNA) and actuating (reconfiguration) can be far from each other. This could be useful in building complex DNA function devices.

The research on deformable DNA structures is rapidly developing yet is still in its youth. Thus, related applications have been relatively limited. Other reviews on the applications of dynamic structures can be found elsewhere.^{48,179-183}

7 CONCLUSIONS AND OUTLOOK

This article provides an overview of the development of DNA nanotechnology, the basic mechanics, and the evolution from static DNA structures to dynamic, deformable nanodevices. We have focused on mechanical perspectives on deformation mechanisms, different scales in modelling, and ultimately design recommendations. Both static and dynamic DNA nanodevices with small deformation share the same basic mechanics, and thus have similar design principles. For a greater degree of deformation (*e.g.*, 10-50% of relative changes), the conformation changes must be considered during the design process. For significant deformation (> 50%), the change of mechanical properties of DNA components must be accounted for as well. Design by parts and iterations on assembled structures are required for complex architectures.

To expand our understanding of dynamic and deformable nanostructures, there are several questions that need to be answered.

What we can build. The dynamic DNA nanostructures with soft ssDNA hinges have been well developed and used for various applications as discussed above. For example, DNA origami boxes have been demonstrated by multiple groups with different chemical schemes;^{112,169,184-186} however, the open-close mechanisms were very similar from the mechanics point of view as all used ssDNA hinges. In contrast, deformations on dsDNA parts are still underdeveloped, yet they could be developed into unique mechanisms for programming structural transformation and functions. This

review summarizes the fundamentals in related mechanics and design suggestions. With a library of mechanical designs and mechanisms, one can envision a broader range of feasible structures and functionalities that may be tailored to specific applications.

How we can program DNA mechanics. In any deformable structures, some parts are designed for structural integrity while the others are accounted for deformation. Under selections of materials with different stiffnesses, distributions of deformation may be arranged. For example, soft parts can deform noticeably, whereas rigid parts may have minimal deformation. The utility of DNA on this aspect is that stiffness of ssDNA is smaller than that of dsDNA by two orders of magnitude.⁵⁹ This can benefit in arranging deformations at different parts. Additional methods include cross-section designs. For example, 6 dsDNA can be arranged into a hexagon or a 3×2 rectangular cross-section. Hexagonal arrangement will have almost the same bending stiffness regardless of bending directions while rectangular lattice will be stiffer if the bending is on the 3-bundle direction and softer if bent on the 2-bundle direction. Depending on the loading, cross-sections should be selected accordingly.

There are several strategies for strengthening DNA, such as adding chemicals that can enhance DNA mechanics. For example, crosslinking molecules can improve the thermal stability of DNA structures,¹²⁶⁻¹²⁹ and will likely enhance the stiffness and mechanical stability. This mechanical enhancement has not been explored yet. Given different crosslinking reactions on different bases (*e.g.*, C and T vs. A and G),^{187,188} it may be possible to design sequence-based stiffness, which could open new opportunities in mechanical designs and related applications. Besides, increasing Na⁺ from 1 mM to 1 M can reduce the DNA stiffness to ~1/3 of the original value.¹⁸⁹ The downside of this salt method is that all the DNA in the structure would be affected. If it is combined with protection methods, such as polyethylene glycol (PEG) coating on DNA, only parts without coating would become softer. As such, DNA may possess 4 distinct rigidities (ssDNA, dsDNA, enhanced DNA, and weakened DNA). This will enable significantly more versatile structures. For example, auxetic DNA origami wireframes may benefit from different stiffness in their designs. Suppose dsDNA edges in the wireframes are replaced with enhanced DNA with higher stiffness. The edges will then be strengthened and likely remain straight during deformation (thus maintaining structural integrity), while the deformability is preserved. Similarly, different rigidities of DNA parts can be used on a structure to enable regioselective deformations during reconfiguration to fit the design purposes.

What we can model. The designs are hinged to the available theoretical and computational models. With new types of deformable structures and several distinct stiffnesses (ssDNA, dsDNA, enhanced DNA, and weakened DNA), dynamic mechanisms and deformation modes can be complex. New models or amendments on available models will be necessary to provide suitable guidance on those structures. For example, crosslinked DNA structures cannot be simulated directly by all-atom models, not to mention the three common models (elasticity theory, FEM, and coarse-grained MD models). Alternatively, the stiffness values of crosslinked double helices could be acquired from experiments, which may then be used as an input for general FEM platforms (*e.g.*, COMSOL). Since the crosslinking typically occurs at designed sites, it will be reasonable to replace the stiffness of those sites with the experimental values in the calculation domain.^{187,188} Therefore, it may be possible for FEM to compute crosslinked structures. One downside of the method is that FEM simulations normally do not reflect the changes of elastic properties under

large deformation. If the structure with enhancement experiences more than small deformation, the simulated results will not be accurate without additional information. One may need to measure the mechanical properties under small and significant deformations for the DNA so that the computation can result in better accuracy. With proper modelling for newly developed structures and mechanical properties, the subfield of dynamic and deformable DNA structures will be on a fast-developing route.

ACKNOWLEDGEMENT

This was supported by the US Department of Energy (award no. DE-SC0020673) and the National Science Foundation (award no. 2025187 and 2134603).

REFERENCE

- 1 Crick, F. Central Dogma of Molecular Biology. *Nature* **227**, 561-563 (1970).
- 2 Seeman, N. C. Nucleic Acid Junctions and Lattices. *Journal of Theoretical Biology* **99**, 237-247 (1982).
- 3 Fu, T. J. & Seeman, N. C. DNA Double-Crossover Molecules. *Biochemistry* **32**, 3211-3220 (1993).
- 4 Li, X., Yang, X., Qi, J. & Seeman, N. C. Antiparallel DNA Double Crossover Molecules As Components for Nanoconstruction. *Journal of the American Chemical Society* **118**, 6131-6140 (1996).
- 5 Yang, X., Wenzler, L. A., Qi, J., Li, X. & Seeman, N. C. Ligation of DNA Triangles Containing Double Crossover Molecules. *Journal of the American Chemical Society* **120**, 9779-9786 (1998).
- 6 Qiu, H., Dewan, J. C. & Seeman, N. C. A DNA Decamer with a Sticky End: The Crystal Structure of d-CGACGATCGT. *Journal of Molecular Biology* **267**, 881-898 (1997).
- 7 Seeman, N. C. DNA in a Material World. *Nature* **421**, 427-431 (2003).
- 8 Aldaye, F. A., Palmer, A. L. & Sleiman, H. F. Assembling Materials with DNA as the Guide. *Science* **321**, 1795-1799 (2008).
- 9 Ke, Y., Ong, L. L., Sun, W., Song, J., Dong, M., Shih, W. M. & Yin, P. DNA Brick Crystals with Prescribed Depths. *Nature Chemistry* **6**, 994-1002 (2014).
- 10 Shih, W. M., Quispe, J. D. & Joyce, G. F. A 1.7-Kilobase Single-Stranded DNA that Folds into a Nanoscale Octahedron. *Nature* **427**, 618-621 (2004).
- 11 Rothemund, P. W. Folding DNA to Create Nanoscale Shapes and Patterns. *Nature* **440**, 297-302 (2006).
- 12 Fan, S., Wang, D., Kenaan, A., Cheng, J., Cui, D. & Song, J. Create Nanoscale Patterns with DNA Origami. *Small* **15**, 1805554 (2019).
- 13 Bila, H., Kurisinkal, E. E. & Bastings, M. M. Engineering a Stable Future for DNA-Origami as a Biomaterial. *Biomaterials Science* **7**, 532-541 (2019).
- 14 Halley, P. D., Patton, R. A., Chowdhury, A., Byrd, J. C. & Castro, C. E. Low-Cost, Simple, and Scalable Self-Assembly of DNA Origami Nanostructures. *Nano Research* **12**, 1207-1215 (2019).
- 15 Chen, H., Cha, T.-G., Pan, J. & Choi, J. H. Hierarchically Assembled DNA Origami Tubules with Reconfigurable Chirality. *Nanotechnology* **24**, 435601 (2013).
- 16 Chen, H., Zhang, H., Pan, J., Cha, T.-G., Li, S., Andréasson, J. & Choi, J. H. Dynamic and Progressive Control of DNA Origami Conformation by Modulating DNA Helicity with Chemical Adducts. *ACS Nano* **10**, 4989-4996 (2016).
- 17 Grome, M. W., Zhang, Z., Pincet, F. & Lin, C. Vesicle Tubulation with Self-Assembling DNA Nanosprings. *Angewandte Chemie International Edition* **57**, 5330-5334 (2018).
- 18 Li, Z., Liu, M., Wang, L., Nangreave, J., Yan, H. & Liu, Y. Molecular Behavior of DNA Origami in Higher-Order Self-Assembly. *Journal of the American Chemical Society* **132**, 13545-13552 (2010).
- 19 Pan, J., Cha, T.-G., Li, F., Chen, H., Bragg, N. A. & Choi, J. H. Visible/Near-Infrared Subdiffraction Imaging Reveals the Stochastic Nature of DNA Walkers. *Science Advances* **3**, e1601600 (2017).
- 20 Du, Y., Pan, J., Qiu, H., Mao, C. & Choi, J. H. Mechanistic Understanding of Surface Migration Dynamics with DNA Walkers. *The Journal of Physical Chemistry B* **125**, 507-517 (2021).

- 21 Jung, C., Allen, P. B. & Ellington, A. D. A Stochastic DNA Walker that Traverses a
Microparticle Surface. *Nature Nanotechnology* **11**, 157-163 (2016).
- 22 Yehl, K., Mugler, A., Vivek, S., Liu, Y., Zhang, Y., Fan, M., Weeks, E. R. & Salaita, K.
High-Speed DNA-Based Rolling Motors Powered by RNase H. *Nature Nanotechnology*
11, 184-190 (2016).
- 23 Yin, P., Yan, H., Daniell, X. G., Turberfield, A. J. & Reif, J. H. A unidirectional DNA
Walker that Moves Autonomously along a Track. *Angewandte Chemie* **116**, 5014-5019
(2004).
- 24 Zhang, F., Nangreave, J., Liu, Y. & Yan, H. Structural DNA Nanotechnology: State of
the Art and Future Perspective. *Journal of the American Chemical Society* **136**, 11198-
11211 (2014).
- 25 Li, F., Cha, T. G., Pan, J., Ozcelikkale, A., Han, B. & Choi, J. H. DNA Walker-Regulated
Cancer Cell Growth Inhibition. *ChemBioChem* **17**, 1138-1141 (2016).
- 26 Tan, W., Wang, K. & Drake, T. J. Molecular Beacons. *Current Opinion in Chemical
Biology* **8**, 547-553 (2004).
- 27 Drake, T. J. & Tan, W. Molecular Beacon DNA Probes and Their Bioanalytical
Applications. *Applied Spectroscopy* **58**, 269A-280A (2004).
- 28 Selnihhin, D., Sparvath, S. M., Preus, S., Birkedal, V. & Andersen, E. S.
Multifluorophore DNA origami beacon as a biosensing platform. *Acs Nano* **12**, 5699-
5708 (2018).
- 29 Zhang, P., Beck, T. & Tan, W. Design of a Molecular Beacon DNA Probe with Two
Fluorophores. *Angewandte Chemie* **113**, 416-419 (2001).
- 30 Fahlman, R. P. & Sen, D. DNA Conformational Switches as Sensitive Electronic Sensors
of Analytes. *Journal of the American Chemical Society* **124**, 4610-4616 (2002).
- 31 Han, D., Kim, Y.-R., Oh, J.-W., Kim, T. H., Mahajan, R. K., Kim, J. S. & Kim, H. A
Regenerative Electrochemical Sensor Based on Oligonucleotide for the Selective
Determination of Mercury (II). *Analyst* **134**, 1857-1862 (2009).
- 32 Li, T., Dong, S. & Wang, E. A Lead(II)-Driven DNA Molecular Device for Turn-On
Fluorescence Detection of Lead(II) Ion with High Selectivity and Sensitivity. *Journal of
the American Chemical Society* **132**, 13156-13157 (2010).
- 33 Wang, F., Liu, X. & Willner, I. DNA Switches: from Principles to Applications.
Angewandte Chemie International Edition **54**, 1098-1129 (2015).
- 34 Xiao, M., Lai, W., Wang, F., Li, L., Fan, C. & Pei, H. Programming Drug Delivery
Kinetics for Active Burst Release with DNA Toehold Switches. *Journal of the American
Chemical Society* **141**, 20354-20364 (2019).
- 35 Xie, C., Hu, Y., Chen, Z., Chen, K. & Pan, L. Tuning curved DNA origami structures
through mechanical design and chemical adducts. *Nanotechnology* (2022).
- 36 Chen, H., Li, R., Li, S., Andréasson, J. & Choi, J. H. Conformational Effects of UV Light
on DNA Origami. *Journal of the American Chemical Society* **139**, 1380-1383 (2017).
- 37 Gopinath, A., Thachuk, C., Mitskovets, A., Atwater, H. A., Kirkpatrick, D. &
Rothemund, P. W. Absolute and Arbitrary Orientation of Single-Molecule Shapes.
Science **371**, eabd6179 (2021).
- 38 Ijäs, H., Shen, B., Heuer-Jungemann, A., Keller, A., Kostianen, M. A., Liedl, T.,
Ihalainen, J. A. & Linko, V. Unraveling the Interaction Between Doxorubicin and DNA
Origami Nanostructures for Customizable Chemotherapeutic Drug Release. *Nucleic
Acids Research* **49**, 3048-3062 (2021).

- 39 Kollmann, F., Ramakrishnan, S., Shen, B., Grundmeier, G., Kostianen, M. A., Linko, V. & Keller, A. Superstructure-Dependent Loading of DNA Origami Nanostructures with a Groove-Binding Drug. *ACS Omega* **3**, 9441-9448 (2018).
- 40 Miller, H. L., Contera, S., Wollman, A. J., Hirst, A., Dunn, K. E., Schröter, S., O'Connell, D. & Leake, M. C. Biophysical Characterisation of DNA Origami Nanostructures Reveals Inaccessibility to Intercalation Binding Sites. *Nanotechnology* **31**, 235605 (2020).
- 41 Zeng, Y., Liu, J., Yang, S., Liu, W., Xu, L. & Wang, R. Time-Lapse Live Cell Imaging to Monitor Doxorubicin Release from DNA Origami Nanostructures. *Journal of Materials Chemistry B* **6**, 1605-1612 (2018).
- 42 Dietz, H., Douglas, S. M. & Shih, W. M. Folding DNA into Twisted and Curved Nanoscale Shapes. *Science* **325**, 725-730 (2009).
- 43 Lee, J. Y., Lee, J. G., Yun, G., Lee, C., Kim, Y.-J., Kim, K. S., Kim, T. H. & Kim, D.-N. Rapid Computational Analysis of DNA Origami Assemblies at Near-Atomic Resolution. *ACS Nano* **15**, 1002-1015 (2021).
- 44 Sun, X., Hyeon Ko, S., Zhang, C., Ribbe, A. E. & Mao, C. Surface-Mediated DNA Self-Assembly. *Journal of the American Chemical Society* **131**, 13248-13249 (2009).
- 45 O'Neill, P., Rothmund, P. W., Kumar, A. & Fygenson, D. K. Sturdier DNA Nanotubes via Ligation. *Nano letters* **6**, 1379-1383 (2006).
- 46 Fujibayashi, K., Hariadi, R., Park, S. H., Winfree, E. & Murata, S. Toward Reliable Algorithmic Self-Assembly of DNA Tiles: A Fixed-Width Cellular Automaton Pattern. *Nano Letters* **8**, 1791-1797 (2008).
- 47 Watson, J. D. & Crick, F. H. Molecular Structure of Nucleic Acids: A Structure for Deoxyribose Nucleic Acid. *Nature* **171**, 737-738 (1953).
- 48 Nummelin, S., Shen, B., Piskunen, P., Liu, Q., Kostianen, M. A. & Linko, V. Robotic DNA Nanostructures. *ACS Synthetic Biology* **9**, 1923-1940 (2020).
- 49 Norton, R. L. *Design of Machinery: an Introduction to the Synthesis and Analysis of Mechanisms and Machines*. (McGraw-Hill/Higher Education, 2008).
- 50 Tadjbakhsh, I. G. Stability of Motion of Elastic Planar Linkages with Application to Slider Crank Mechanism. *Journal of Mechanical Design* **104**, 698-703 (1982).
- 51 Brodell, R. J. & Soni, A. Design of the Crank-Rocker Mechanism with Unit Time Ratio. *Journal of Mechanisms* **5**, 1-4 (1970).
- 52 Mabie, H. H. & Reinholtz, C. F. *Mechanisms and Dynamics of Machinery*. (John Wiley & Sons, 1991).
- 53 Boal, D. *Mechanics of the Cell*. (Cambridge University Press, 2012).
- 54 Chen, H., Weng, T.-W., Riccitelli, M. M., Cui, Y., Irudayaraj, J. & Choi, J. H. Understanding the Mechanical Properties of DNA Origami Tiles and Controlling the Kinetics of Their Folding and Unfolding Reconfiguration. *Journal of the American Chemical Society* **136**, 6995-7005 (2014).
- 55 Marko, J. F. & Cocco, S. The Micromechanics of DNA. *Physics World* **16**, 37 (2003).
- 56 Kim, D.-N., Kilchherr, F., Dietz, H. & Bathe, M. Quantitative Prediction of 3D Solution Shape and Flexibility of Nucleic Acid Nanostructures. *Nucleic Acids Research* **40**, 2862-2868 (2012).
- 57 Snodin, B. E., Randisi, F., Mosayebi, M., Šulc, P., Schreck, J. S., Romano, F., Ouldrige, T. E., Tsukanov, R., Nir, E. & Louis, A. A. Introducing Improved Structural Properties

- and Salt Dependence into a Coarse-Grained Model of DNA. *The Journal of Chemical Physics* **142**, 234901 (2015).
- 58 Crandall, S. H., Dahl, N. C. & Lardner, T. *An Introduction to the Mechanics of Solids, 3rd Edn; SI Units*. (McGraw-Hill Book Company, 2012).
- 59 Hays, J. B. & Zimm, B. H. Flexibility and Stiffness in Nicked DNA. *Journal of Molecular Biology* **48**, 297-317 (1970).
- 60 Johnston, E. R. J., DeWolf, J. T. & Beer, F. P. *Mechanics of Materials*. (McGraw-Hill, 2001).
- 61 Berengut, J. F., Wong, C. K., Berengut, J. C., Doye, J. P., Ouldridge, T. E. & Lee, L. K. Self-Limiting Polymerization of DNA Origami Subunits with Strain Accumulation. *ACS Nano* **14**, 17428-17441 (2020).
- 62 Wagenbauer, K. F., Sigl, C. & Dietz, H. Gigadalton-Scale Shape-Programmable DNA Assemblies. *Nature* **552**, 78-83 (2017).
- 63 Kauert, D. J., Kurth, T., Liedl, T. & Seidel, R. Direct Mechanical Measurements Reveal the Material Properties of Three-Dimensional DNA Origami. *Nano Letters* **11**, 5558-5563 (2011).
- 64 Ke, Y., Douglas, S. M., Liu, M., Sharma, J., Cheng, A., Leung, A., Liu, Y., Shih, W. M. & Yan, H. Multilayer DNA Origami Packed on a Square Lattice. *Journal of the American Chemical Society* **131**, 15903-15908 (2009).
- 65 Ke, Y., Voigt, N. V., Gothelf, K. V. & Shih, W. M. Multilayer DNA Origami Packed on Hexagonal and Hybrid Lattices. *Journal of the American Chemical Society* **134**, 1770-1774 (2012).
- 66 Castro, C. E., Kilchherr, F., Kim, D.-N., Shiao, E. L., Wauer, T., Wortmann, P., Bathe, M. & Dietz, H. A Primer to Scaffolded DNA Origami. *Nature Methods* **8**, 221-229 (2011).
- 67 Han, D., Pal, S., Yang, Y., Jiang, S., Nangreave, J., Liu, Y. & Yan, H. DNA Gridiron Nanostructures Based on Four-Arm Junctions. *Science* **339**, 1412-1415 (2013).
- 68 Zhang, F., Jiang, S., Wu, S., Li, Y., Mao, C., Liu, Y. & Yan, H. Complex Wireframe DNA Origami Nanostructures with Multi-Arm Junction Vertices. *Nature Nanotechnology* **10**, 779-784 (2015).
- 69 Simmel, S. S., Nickels, P. C. & Liedl, T. Wireframe and Tensegrity DNA Nanostructures. *Accounts of Chemical Research* **47**, 1691-1699 (2014).
- 70 Jun, H., Wang, X., Parsons, M. F., Bricker, W. P., John, T., Li, S., Jackson, S., Chiu, W. & Bathe, M. Rapid Prototyping of Arbitrary 2D and 3D Wireframe DNA Origami. *Nucleic Acids Research* **49**, 10265-10274 (2021).
- 71 Wang, X., Jun, H. & Bathe, M. Programming 2D Supramolecular Assemblies with Wireframe DNA Origami. *Journal of the American Chemical Society* **144**, 4403-4409 (2022).
- 72 Wang, W., Chen, S., An, B., Huang, K., Bai, T., Xu, M., Bellot, G., Ke, Y., Xiang, Y. & Wei, B. Complex Wireframe DNA Nanostructures from Simple Building Blocks. *Nature Communications* **10**, 1-8 (2019).
- 73 Jun, H., Zhang, F., Shepherd, T., Ratanalert, S., Qi, X., Yan, H. & Bathe, M. Autonomously Designed Free-Form 2D DNA Origami. *Science Advances* **5**, eaav0655 (2019).
- 74 Yin, P., Hariadi, R. F., Sahu, S., Choi, H. M., Park, S. H., LaBean, T. H. & Reif, J. H. Programming DNA Tube Circumferences. *Science* **321**, 824-826 (2008).

- 75 Ke, Y., Liu, Y., Zhang, J. & Yan, H. A study of DNA Tube Formation Mechanisms Using 4-, 8-, and 12-Helix DNA Nanostructures. *Journal of the American Chemical Society* **128**, 4414-4421 (2006).
- 76 Douglas, S. M., Marblestone, A. H., Teerapittayanon, S., Vazquez, A., Church, G. M. & Shih, W. M. Rapid Prototyping of 3D DNA-Origami Shapes with CaDNAno. *Nucleic Acids Research* **37**, 5001-5006 (2009).
- 77 Aggarwal, A., Naskar, S., Sahoo, A. K., Mogurampelly, S., Garai, A. & Maiti, P. K. What do We Know about DNA Mechanics so far? *Current Opinion in Structural Biology* **64**, 42-50 (2020).
- 78 Jun, H., Wang, X., Bricker, W. P. & Bathe, M. Automated Sequence Design of 2D Wireframe DNA origami with Honeycomb Edges. *Nature Communications* **10**, 1-9 (2019).
- 79 He, Y., Ye, T., Su, M., Zhang, C., Ribbe, A. E., Jiang, W. & Mao, C. Hierarchical Self-assembly of DNA into Symmetric Supramolecular Polyhedra. *Nature* **452**, 198-201 (2008).
- 80 Ko, S. H., Su, M., Zhang, C., Ribbe, A. E., Jiang, W. & Mao, C. Synergistic Self-Assembly of RNA and DNA Molecules. *Nature Chemistry* **2**, 1050-1055 (2010).
- 81 Ong, L. L., Hanikel, N., Yaghi, O. K., Grun, C., Strauss, M. T., Bron, P., Lai-Kee-Him, J., Schueder, F., Wang, B. & Wang, P. Programmable Self-Assembly of Three-Dimensional Nanostructures from 10,000 Unique Components. *Nature* **552**, 72-77 (2017).
- 82 Zheng, J., Birktoft, J. J., Chen, Y., Wang, T., Sha, R., Constantinou, P. E., Ginell, S. L., Mao, C. & Seeman, N. C. From Molecular to Macroscopic via the Rational Design of a Self-Assembled 3D DNA Crystal. *Nature* **461**, 74-77 (2009).
- 83 Simmons, C. R., Zhang, F., Birktoft, J. J., Qi, X., Han, D., Liu, Y., Sha, R., Abdallah, H. O., Hernandez, C., Ohayon, Y. P., Seeman, N. C. & Yan, H. Construction and Structure Determination of a Three-Dimensional DNA Crystal. *Journal of the American Chemical Society* **138**, 10047-10054 (2016).
- 84 Zhang, F., Simmons, C. R., Gates, J., Liu, Y. & Yan, H. Self-Assembly of a 3D DNA Crystal Structure with Rationally Designed Six-Fold Symmetry. *Angewandte Chemie International Edition* **57**, 12504-12507 (2018).
- 85 Li, Z., Liu, L., Zheng, M., Zhao, J., Seeman, N. C. & Mao, C. Making Engineered 3D DNA Crystals Robust. *Journal of the American Chemical Society* **141**, 15850-15855 (2019).
- 86 Liu, M., Fu, J., Hejesen, C., Yang, Y., Woodbury, N. W., Gothelf, K., Liu, Y. & Yan, H. A DNA Tweezer-Actuated Enzyme Nanoreactor. *Nature Communications* **4**, 1-5 (2013).
- 87 Yurke, B., Turberfield, A. J., Mills, A. P., Simmel, F. C. & Neumann, J. L. A DNA-Fuelled Molecular Machine Made of DNA. *Nature* **406**, 605-608 (2000).
- 88 Wang, D., Song, J., Wang, P., Pan, V., Zhang, Y., Cui, D. & Ke, Y. Design and Operation of Reconfigurable Two-Dimensional DNA Molecular Arrays. *Nature Protocols* **13**, 2312-2329 (2018).
- 89 Deng, J. & Walther, A. Pathway Complexity in Fuel-Driven DNA Nanostructures with Autonomous Reconfiguration of Multiple Dynamic Steady States. *Journal of the American Chemical Society* **142**, 685-689 (2020).
- 90 Ke, Y., Meyer, T., Shih, W. M. & Bellot, G. Regulation at a Distance of Biomolecular Interactions Using a DNA Origami Nanoactuator. *Nature Communications* **7**, 1-8 (2016).

- 91 Han, D., Huang, J., Zhu, Z., Yuan, Q., You, M., Chen, Y. & Tan, W. Molecular Engineering of Photoresponsive Three-Dimensional DNA Nanostructures. *Chemical Communications* **47**, 4670-4672 (2011).
- 92 Zhou, C., Xin, L., Duan, X., Urban, M. J. & Liu, N. Dynamic Plasmonic System that Responds to Thermal and Aptamer-Target Regulations. *Nano Letters* **18**, 7395-7399 (2018).
- 93 Li, R., Chen, H. & Choi, J. H. Auxetic Two-Dimensional Nanostructures from DNA. *Angewandte Chemie International Edition* **60**, 7165-7173 (2021).
- 94 Zhan, P., Dutta, P. K., Wang, P., Song, G., Dai, M., Zhao, S.-X., Wang, Z.-G., Yin, P., Zhang, W. & Ding, B. Reconfigurable Three-Dimensional Gold Nanorod Plasmonic Nanostructures Organized on DNA Origami Tripod. *ACS Nano* **11**, 1172-1179 (2017).
- 95 Wang, D., Yu, L., Huang, C.-M., Arya, G., Chang, S. & Ke, Y. Programmable Transformations of DNA Origami Made of Small Modular Dynamic Units. *Journal of the American Chemical Society* **143**, 2256-2263 (2021).
- 96 Goodman, R. P., Heilemann, M., Doose, S., Erben, C. M., Kapanidis, A. N. & Turberfield, A. J. Reconfigurable, Braced, Three-Dimensional DNA Nanostructures. *Nature Nanotechnology* **3**, 93-96 (2008).
- 97 Aldaye, F. A. & Sleiman, H. F. Modular Access to Structurally Switchable 3D Discrete DNA Assemblies. *Journal of the American Chemical Society* **129**, 13376-13377 (2007).
- 98 Choi, Y., Choi, H., Lee, A. C., Lee, H. & Kwon, S. A Reconfigurable DNA Accordion Rack. *Angewandte Chemie International Edition* **57**, 2811-2815 (2018).
- 99 Wang, W., Chen, C., Vecchioni, S., Zhang, T., Wu, C., Ohayon, Y. P., Sha, R., Seeman, N. C. & Wei, B. Reconfigurable Two-Dimensional DNA Lattices: Static and Dynamic Angle Control. *Angewandte Chemie* **133**, 25985-25990 (2021).
- 100 Pfitzner, E., Wachauf, C., Kilchherr, F., Pelz, B., Shih, W. M., Rief, M. & Dietz, H. Rigid DNA Beams for High-Resolution Single-Molecule Mechanics. *Angewandte Chemie International Edition* **52**, 7766-7771 (2013).
- 101 Wang, M. D., Yin, H., Landick, R., Gelles, J. & Block, S. M. Stretching DNA with Optical Tweezers. *Biophysical Journal* **72**, 1335-1346 (1997).
- 102 Bockelmann, U., Thomen, P., Essevez-Roulet, B., Viasnoff, V. & Heslot, F. Unzipping DNA with Optical Tweezers: High Sequence Sensitivity and Force Flips. *Biophysical Journal* **82**, 1537-1553 (2002).
- 103 Xin, Q., Li, P., He, Y., Shi, C., Qiao, Y., Bian, X., Su, J., Qiao, R., Zhou, X. & Zhong, J. Magnetic Tweezers for the Mechanical Research of DNA at the Single Molecule Level. *Analytical Methods* **9**, 5720-5730 (2017).
- 104 Yan, J., Skoko, D. & Marko, J. F. Near-Field-Magnetic-Tweezer Manipulation of Single DNA Molecules. *Physical Review E* **70**, 011905 (2004).
- 105 Gao, M., Hu, J., Wang, Y., Liu, M., Wang, J., Song, Z., Xu, H., Hu, C. & Wang, Z. Controlled Self-Assembly of λ -DNA Networks with the Synergistic Effect of a DC Electric Field. *The Journal of Physical Chemistry B* **123**, 9809-9818 (2019).
- 106 Kopperger, E., List, J., Madhira, S., Rothfischer, F., Lamb, D. C. & Simmel, F. C. A Self-Assembled Nanoscale Robotic Arm Controlled by Electric Fields. *Science* **359**, 296-301 (2018).
- 107 Zheng, L., Brody, J. P. & Burke, P. J. Electronic Manipulation of DNA, Proteins, and Nanoparticles for Potential Circuit Assembly. *Biosensors and Bioelectronics* **20**, 606-619 (2004).

- 108 Li, R., Zheng, M., Madhavacharyula, A. S., Du, Y., Mao, C. & Choi, J. H. Mechanical Deformation Behaviors and Structural Properties of Ligated DNA Crystals. *Biophysical Journal*, doi:10.1016/j.bpj.2022.09.036 (2022).
- 109 Zhou, F., Sun, W., Zhang, C., Shen, J., Yin, P. & Liu, H. 3D Freestanding DNA Nanostructure Hybrid as a Low-Density High-Strength Material. *ACS Nano* **14**, 6582-6588 (2020).
- 110 Ma, Z., Kim, Y.-J., Park, S., Hirai, Y., Tsuchiya, T., Kim, D.-N. & Tabata, O. in *10th IEEE International Conference on Nano/Micro Engineered and Molecular Systems*. 581-584 (IEEE).
- 111 Zhang, Z., Yang, Y., Pincet, F., Llaguno, M. C. & Lin, C. Placing and Shaping Liposomes with Reconfigurable DNA Nanocages. *Nature Chemistry* **9**, 653-659 (2017).
- 112 Andersen, E. S., Dong, M., Nielsen, M. M., Jahn, K., Subramani, R., Mamdouh, W., Golas, M. M., Sander, B., Stark, H., Oliveira, C. L., Pedersen, J. S., Birkedal, V., Besenbacher, F., Gothelf, K. V. & Kjems, J. Self-Assembly of a Nanoscale DNA Box with a Controllable Lid. *Nature* **459**, 73-76 (2009).
- 113 Sannohe, Y., Endo, M., Katsuda, Y., Hidaka, K. & Sugiyama, H. Visualization of Dynamic Conformational Switching of the G-Quadruplex in a DNA Nanostructure. *Journal of the American Chemical Society* **132**, 16311-16313 (2010).
- 114 Torelli, E., Marini, M., Palmano, S., Piantanida, L., Polano, C., Scarpellini, A., Lazzarino, M. & Firrao, G. A DNA Origami Nanorobot Controlled by Nucleic Acid Hybridization. *Small* **10**, 2918-2926 (2014).
- 115 Ijäs, H., Hakaste, I., Shen, B., Kostianen, M. A. & Linko, V. Reconfigurable DNA Origami Nanocapsule for pH-Controlled Encapsulation and Display of Cargo. *ACS Nano* **13**, 5959-5967 (2019).
- 116 Jiang, Q., Liu, Q., Shi, Y., Wang, Z.-G., Zhan, P., Liu, J., Liu, C., Wang, H., Shi, X. & Zhang, L. Stimulus-Responsive Plasmonic Chiral Signals of Gold Nanorods Organized on DNA Origami. *Nano Letters* **17**, 7125-7130 (2017).
- 117 Saccà, B., Ishitsuka, Y., Meyer, R., Sprengel, A., Schöneweiß, E. C., Nienhaus, G. U. & Niemeyer, C. M. Reversible Reconfiguration of DNA Origami Nanochambers Monitored by Single-Molecule FRET. *Angewandte Chemie International Edition* **54**, 3592-3597 (2015).
- 118 Kuzuya, A., Watanabe, R., Hashizume, M., Kaino, M., Minamida, S., Kameda, K. & Ohya, Y. Precise Structure Control of Three-State Nanomechanical DNA Origami Devices. *Methods* **67**, 250-255 (2014).
- 119 Gibson, L. J. & Ashby, M. F. *Cellular Solids: Structure and Properties*. (Cambridge University Press, 1999).
- 120 Gür, F. N., Schwarz, F. W., Ye, J., Diez, S. & Schmidt, T. L. Toward Self-Assembled Plasmonic Devices: High-Yield Arrangement of Gold Nanoparticles on DNA Origami Templates. *ACS Nano* **10**, 5374-5382 (2016).
- 121 Jiang, Q., Shi, Y., Zhang, Q., Li, N., Zhan, P., Song, L., Dai, L., Tian, J., Du, Y. & Cheng, Z. A Self-Assembled DNA Origami-Gold Nanorod Complex for Cancer Theranostics. *Small* **11**, 5134-5141 (2015).
- 122 Song, L., Jiang, Q., Liu, J., Li, N., Liu, Q., Dai, L., Gao, Y., Liu, W., Liu, D. & Ding, B. DNA Origami/Gold Nanorod Hybrid Nanostructures for the Circumvention of Drug Resistance. *Nanoscale* **9**, 7750-7754 (2017).

- 123 Szaciłowski, K., Macyk, W., Drzewiecka-Matuszek, A., Brindell, M. & Stochel, G. Bioinorganic photochemistry: frontiers and mechanisms. *Chemical reviews* **105**, 2647-2694 (2005).
- 124 Di Pietro, M. L., Puntoriero, F., Tuyéras, F., Ochsenein, P., Lainé, P. P. & Campagna, S. Photochemically Driven Intercalation of Small Molecules into DNA by In Situ Irradiation. *Chemical Communications* **46**, 5169-5171 (2010).
- 125 Zou, S., Lei, Y., Ma, W., Chen, B., Cheng, H., Jia, R., Li, Z., He, X. & Wang, K. Extracellular pH-manipulated in situ reconfiguration of aptamer functionalized DNA monomer enables specifically improved affinity, detection and drug delivery. *Analyst* **145**, 2562-2569 (2020).
- 126 Gerling, T., Kube, M., Kick, B. & Dietz, H. Sequence-programmable covalent bonding of designed DNA assemblies. *Science advances* **4**, eaau1157 (2018).
- 127 Rajendran, A., Endo, M., Katsuda, Y., Hidaka, K. & Sugiyama, H. Photo-Cross-Linking-Assisted Thermal Stability of DNA Origami Structures and its Application for Higher-Temperature Self-Assembly. *Journal of the American Chemical Society* **133**, 14488-14491 (2011).
- 128 Anastassacos, F. M., Zhao, Z., Zeng, Y. & Shih, W. M. Glutaraldehyde Cross-Linking of Oligolysines Coating DNA Origami Greatly Reduces Susceptibility to Nuclease Degradation. *Journal of the American Chemical Society* **142**, 3311-3315 (2020).
- 129 Sala, L., Perecko, T., Mestek, O., Pinkas, D., Homola, T. s. & Kočišek, J. Cisplatin-Cross-Linked DNA Origami Nanostructures for Drug Delivery Applications. *ACS Applied Nano Materials* (2022).
- 130 Jungmann, R., Scheible, M. & Simmel, F. C. Nanoscale Imaging in DNA Nanotechnology. *WIREs Nanomedicine and Nanobiotechnology* **4**, 66-81 (2012).
- 131 Garcia, R. Nanomechanical Mapping of Soft Materials with the Atomic Force Microscope: Methods, Theory and Applications. *Chemical Society Reviews* **49**, 5850-5884 (2020).
- 132 Li, F., Chen, H., Pan, J., Cha, T.-G., Medintz, I. L. & Choi, J. H. A DNzyme-Mediated Logic Gate for Programming Molecular Capture and Release on DNA Origami. *Chemical Communications* **52**, 8369-8372 (2016).
- 133 Heenan, P. R. & Perkins, T. T. Imaging DNA Equilibrated onto Mica in Liquid Using Biochemically Relevant Deposition Conditions. *ACS Nano* **13**, 4220-4229 (2019).
- 134 Zhang, F., Nangreave, J., Liu, Y. & Yan, H. Reconfigurable DNA Origami to Generate Quasifractal Patterns. *Nano letters* **12**, 3290-3295 (2012).
- 135 Liu, H., Chen, Y., He, Y., Ribbe, A. E. & Mao, C. Approaching the Limit: Can One DNA Oligonucleotide Assemble into Large Nanostructures? *Angewandte Chemie International Edition* **45**, 1942-1945 (2006).
- 136 Kielar, C., Ramakrishnan, S., Fricke, S., Grundmeier, G. & Keller, A. Dynamics of DNA Origami Lattice Formation at Solid-Liquid Interfaces. *ACS Applied Materials & Interfaces* **10**, 44844-44853 (2018).
- 137 Endo, M. Surface Assembly of DNA Origami on a Lipid Bilayer Observed Using High-Speed Atomic Force Microscopy. *Molecules* **27**, 4224 (2022).
- 138 Yang, Y., Tashiro, R., Suzuki, Y., Emura, T., Hidaka, K., Sugiyama, H. & Endo, M. A Photoregulated DNA-Based Rotary System and Direct Observation of its Rotational Movement. *Chemistry – A European Journal* **23**, 3979-3985 (2017).

- 139 Stamov, D. R., Neumann, T., Kraus, A., Körnig, A., Jankowski, T., Knebel, D., Jähnke, T., Henze, T. & Haschke, H. Unraveling Molecular Dynamics with High-Speed Video-Rate Atomic Force Microscopy. *Microscopy Today* **30**, 10-14 (2022).
- 140 Endo, M. & Sugiyama, H. Single-Molecule Imaging of Dynamic Motions of Biomolecules in DNA Origami Nanostructures Using High-Speed Atomic Force Microscopy. *Accounts of Chemical Research* **47**, 1645-1653 (2014).
- 141 Andersen, E. S., Dong, M., Nielsen, M. M., Jahn, K., Lind-Thomsen, A., Mamdouh, W., Gothelf, K. V., Besenbacher, F. & Kjems, J. DNA Origami Design of Dolphin-Shaped Structures with Flexible Tails. *ACS Nano* **2**, 1213-1218 (2008).
- 142 Li, L., Zhang, P., Li, J., Wang, Y., Wei, Y., Hu, J., Zhou, X., Xu, B. & Li, B. Measurement of Nanomechanical Properties of DNA Molecules by PeakForce Atomic Force Microscopy Based on DNA Origami. *Nanoscale* **11**, 4707-4711 (2019).
- 143 Thamm, S., Slesiona, N., Dathe, A., Csáki, A. & Fritzsche, W. AFM-Based Probing of the Flexibility and Surface Attachment of Immobilized DNA Origami. *Langmuir* **34**, 15093-15098 (2018).
- 144 Bai, X.-c., Martin, T. G., Scheres, S. H. & Dietz, H. Cryo-EM Structure of a 3D DNA-Origami Object. *Proceedings of the National Academy of Sciences* **109**, 20012-20017 (2012).
- 145 Jun, H., Shepherd, T. R., Zhang, K., Bricker, W. P., Li, S., Chiu, W. & Bathe, M. Automated Sequence Design of 3D Polyhedral Wireframe DNA Origami with Honeycomb Edges. *ACS Nano* **13**, 2083-2093 (2019).
- 146 Zhou, L., Marras, A. E., Su, H.-J. & Castro, C. E. DNA Origami Compliant Nanostructures with Tunable Mechanical Properties. *ACS Nano* **8**, 27-34 (2014).
- 147 Thubagere, A. J., Li, W., Johnson, R. F., Chen, Z., Doroudi, S., Lee, Y. L., Izatt, G., Wittman, S., Srinivas, N. & Woods, D. A Cargo-Sorting DNA Robot. *Science* **357**, eaan6558 (2017).
- 148 Du, Y., Pan, J. & Choi, J. H. A Review on Optical Imaging of DNA Nanostructures and Dynamic Processes. *Methods and Applications in Fluorescence* **7**, 012002 (2019).
- 149 Algar, W. R., Hildebrandt, N., Vogel, S. S. & Medintz, I. L. FRET as a Biomolecular Research Tool — Understanding its Potential While Avoiding Pitfalls. *Nature Methods* **16**, 815-829 (2019).
- 150 Qiu, H., Li, F., Du, Y., Li, R., Hyun, J. Y., Lee, S. Y. & Choi, J. H. Programmable Aggregation of Artificial Cells with DNA Signals. *ACS Synthetic Biology* **10**, 1268-1276 (2021).
- 151 Schnitzbauer, J., Strauss, M. T., Schlichthaerle, T., Schueder, F. & Jungmann, R. Super-Resolution Microscopy with DNA-PAINT. *Nature Protocols* **12**, 1198-1228 (2017).
- 152 Jungmann, R., Avendaño, M. S., Woehrstein, J. B., Dai, M., Shih, W. M. & Yin, P. Multiplexed 3D Cellular Super-Resolution Imaging with DNA-PAINT and Exchange-PAINT. *Nature Methods* **11**, 313-318 (2014).
- 153 Wade, O. K., Woehrstein, J. B., Nickels, P. C., Strauss, S., Stehr, F., Stein, J., Schueder, F., Strauss, M. T., Ganji, M. & Schnitzbauer, J. 124-Color Super-Resolution Imaging by Engineering DNA-PAINT Blinking Kinetics. *Nano Letters* **19**, 2641-2646 (2019).
- 154 Schueder, F., Stein, J., Stehr, F., Auer, A., Sperl, B., Strauss, M. T., Schwille, P. & Jungmann, R. An Order of Magnitude Faster DNA-PAINT Imaging by Optimized Sequence Design and Buffer Conditions. *Nature Methods* **16**, 1101-1104 (2019).

- 155 Iinuma, R., Ke, Y., Jungmann, R., Schlichthaerle, T., Woehrstein, J. B. & Yin, P. Polyhedra Self-Assembled from DNA Tripods and Characterized with 3D DNA-PAINT. *Science* **344**, 65-69 (2014).
- 156 Gittes, F. & Schmidt, C. F. Interference Model for Back-Focal-Plane Displacement Detection in Optical Tweezers. *Optics Letters* **23**, 7-9 (1998).
- 157 Smith, S. B., Cui, Y. & Bustamante, C. Overstretching B-DNA: The Elastic Response of Individual Double-Stranded and Single-Stranded DNA Molecules. *Science* **271**, 795-799 (1996).
- 158 Heng, J. B., Aksimentiev, A., Ho, C., Marks, P., Grinkova, Y. V., Sligar, S., Schulten, K. & Timp, G. Stretching DNA Using the Electric Field in a Synthetic Nanopore. *Nano Letters* **5**, 1883-1888 (2005).
- 159 Pumm, A.-K., Engelen, W., Kopperger, E., Isensee, J., Vogt, M., Kozina, V., Kube, M., Honemann, M. N., Bertosin, E. & Langecker, M. A DNA Origami Rotary Ratchet Motor. *Nature* **607**, 492-498 (2022).
- 160 Li, R., Chen, H., Lee, H. & Choi, J. H. Elucidating the Mechanical Energy for Cyclization of a DNA Origami Tile. *Applied Sciences* **11**, 2357 (2021).
- 161 Marras, A. E., Zhou, L., Su, H.-J. & Castro, C. E. Programmable Motion of DNA Origami Mechanisms. *Proceedings of the National Academy of Sciences* **112**, 713-718 (2015).
- 162 Kuhn, W. Über die Gestalt fadenförmiger Moleküle in Lösungen. *Kolloid-Zeitschrift* **68**, 2-15 (1934).
- 163 Kratky, O. & Porod, G. Röntgenuntersuchung Gelöster Fadenmoleküle. *Recueil des Travaux Chimiques des Pays -Bas* **68**, 1106-1122 (1949).
- 164 Balabaev, N. & Khazanovich, T. Extension of Chains Composed of Freely Joined Elastic Segments. *Russian Journal of Physical Chemistry B* **3**, 242-246 (2009).
- 165 Engel, M. C., Romano, F., Louis, A. A. & Doye, J. P. Measuring Internal Forces in Single-Stranded DNA: Application to a DNA Force Clamp. *Journal of Chemical Theory and Computation* **16**, 7764-7775 (2020).
- 166 Phillips, J. C., Hardy, D. J., Maia, J. D., Stone, J. E., Ribeiro, J. V., Bernardi, R. C., Buch, R., Fiorin, G., Hénin, J. & Jiang, W. Scalable Molecular Dynamics on CPU and GPU Architectures with NAMD. *The Journal of Chemical Physics* **153**, 044130 (2020).
- 167 Hübner, K., Joshi, H., Aksimentiev, A., Stefani, F. D., Tinnefeld, P. & Acuna, G. P. Determining the in-Plane Orientation and Binding Mode of Single Fluorescent Dyes in DNA origami structures. *ACS Nano* **15**, 5109-5117 (2021).
- 168 Huang, C.-M., Kucinic, A., Johnson, J. A., Su, H.-J. & Castro, C. E. Integrated Computer-Aided Engineering and Design for DNA Assemblies. *Nature Materials* **20**, 1264-1271 (2021).
- 169 Zadegan, R. M., Jepsen, M. D., Thomsen, K. E., Okholm, A. H., Schaffert, D. H., Andersen, E. S., Birkedal, V. & Kjems, J. Construction of a 4 Zeptoliters Switchable 3D DNA Box Origami. *ACS Nano* **6**, 10050-10053 (2012).
- 170 Douglas, S. M., Bachelet, I. & Church, G. M. A Logic-Gated Nanorobot for Targeted Transport of Molecular Payloads. *Science* **335**, 831-834 (2012).
- 171 Tang, Z., Shangguan, D., Wang, K., Shi, H., Sefah, K., Mallikratchy, P., Chen, H. W., Li, Y. & Tan, W. Selection of Aptamers for Molecular Recognition and Characterization of Cancer Cells. *Analytical Chemistry* **79**, 4900-4907 (2007).

- 172 Huang, Y. F., Shangguan, D., Liu, H., Phillips, J. A., Zhang, X., Chen, Y. & Tan, W. Molecular Assembly of an Aptamer–Drug Conjugate for Targeted Drug Delivery to Tumor Cells. *ChemBioChem* **10**, 862-868 (2009).
- 173 Yang, Y., Wang, J., Shigematsu, H., Xu, W., Shih, W. M., Rothman, J. E. & Lin, C. Self-Assembly of Size-Controlled Liposomes on DNA Nanotemplates. *Nature Chemistry* **8**, 476-483 (2016).
- 174 Li, R., Chen, H. & Choi, J. H. Topological Assembly of a Deployable Hoberman Flight Ring from DNA. *Small* **17**, 2007069 (2021).
- 175 Li, R., Yao, Y.-A. & Kong, X. A Class of Reconfigurable Deployable Platonic Mechanisms. *Mechanism and Machine Theory* **105**, 409-427 (2016).
- 176 Speir, J. A., Munshi, S., Wang, G., Baker, T. S. & Johnson, J. E. Structures of the Native and Swollen Forms of Cowpea Chlorotic Mottle Virus Determined by X-Ray Crystallography and Cryo-Electron Microscopy. *Structure* **3**, 63-78 (1995).
- 177 Tama, F. & Brooks III, C. L. The Mechanism and Pathway of pH Induced Swelling in Cowpea Chlorotic Mottle Virus. *Journal of Molecular Biology* **318**, 733-747 (2002).
- 178 Song, J., Li, Z., Wang, P., Meyer, T., Mao, C. & Ke, Y. Reconfiguration of DNA Molecular Arrays Driven by Information Relay. *Science* **357**, eaan3377 (2017).
- 179 Ji, J., Karna, D. & Mao, H. DNA Origami Nano-Mechanics. *Chemical Society Reviews* (2021).
- 180 Ke, Y., Castro, C. & Choi, J. H. Structural DNA Nanotechnology: Artificial Nanostructures for Biomedical Research. *Annual Review of Biomedical Engineering* **20** (2018).
- 181 He, L., Mu, J., Gang, O. & Chen, X. Rationally Programming Nanomaterials with DNA for Biomedical Applications. *Advanced Science* **8**, 2003775 (2021).
- 182 Keller, A. & Linko, V. Challenges and Perspectives of DNA Nanostructures in Biomedicine. *Angewandte Chemie International Edition* **59**, 15818-15833 (2020).
- 183 Ramezani, H. & Dietz, H. Building Machines with DNA Molecules. *Nature Reviews Genetics* **21**, 5-26 (2020).
- 184 Burns, J. R., Lamarre, B., Pyne, A. L., Noble, J. E. & Ryadnov, M. G. DNA Origami Inside-Out Viruses. *ACS Synthetic Biology* **7**, 767-773 (2018).
- 185 Kuzuya, A. & Komiyama, M. Design and Construction of a Box-Shaped 3D-DNA Origami. *Chemical Communications*, 4182-4184 (2009).
- 186 Ranjbar, R. & Hafezi-Moghadam, M. S. Design and Construction of a DNA Origami Drug Delivery System Based on MPT64 Antibody Aptamer for Tuberculosis Treatment. *Electronic Physician* **8**, 1857 (2016).
- 187 Lo, H.-L., Nakajima, S., Ma, L., Walter, B., Yasui, A., Ethell, D. W. & Owen, L. B. Differential Biologic Effects of CPD and 6-4PP UV-Induced DNA Damage on the Induction of Apoptosis and Cell-Cycle Arrest. *BMC Cancer* **5**, 135 (2005).
- 188 Scrima, A., Koničková, R., Czyzewski, B. K., Kawasaki, Y., Jeffrey, P. D., Groisman, R., Nakatani, Y., Iwai, S., Pavletich, N. P. & Thomä, N. H. Structural Basis of UV DNA-Damage Recognition by the DDB1–DDB2 Complex. *Cell* **135**, 1213-1223 (2008).
- 189 Hagerman, P. J. Flexibility of DNA. *Annual Review of Biophysics and Biophysical Chemistry* **17**, 265-286 (1988).
- 190 Bustamante, C., Bryant, Z. & Smith, S. B. Ten Years of Tension: Single-Molecule DNA Mechanics. *Nature* **421**, 423-427 (2003).

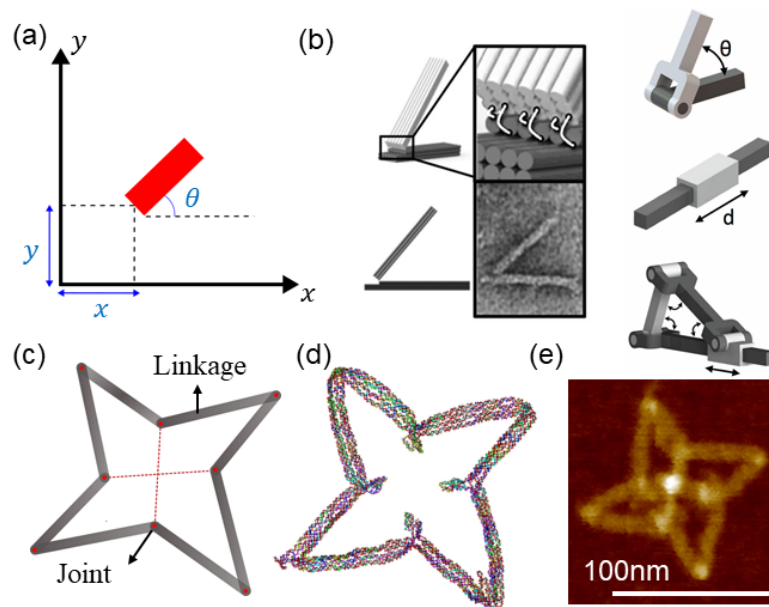


Figure 1. (a) A planar rigid body with 3 degrees of freedom (DOF), *i.e.*, the coordinates x , y , and the angle of inclination θ . (b) An example of common kinematic mechanisms and a nanoscale hinge realized using ssDNA connections (white lines in the inset).¹⁶¹ The transmission electron microscopy (TEM) image resembles the design. On the right side, angular (top), linear (middle), and combined motions are shown in schematics. (c)-(e) Architected auxetic metastructures from DNA.⁹³ (c) Schematic of a unit cell of a rotating square design composed of linkages and joints. (d) Coarse-grained molecular dynamics (MD) simulation on the oxDNA platform and (e) Atomic force microscopy (AFM) image of the DNA origami unit. Scale bar: 100 nm.

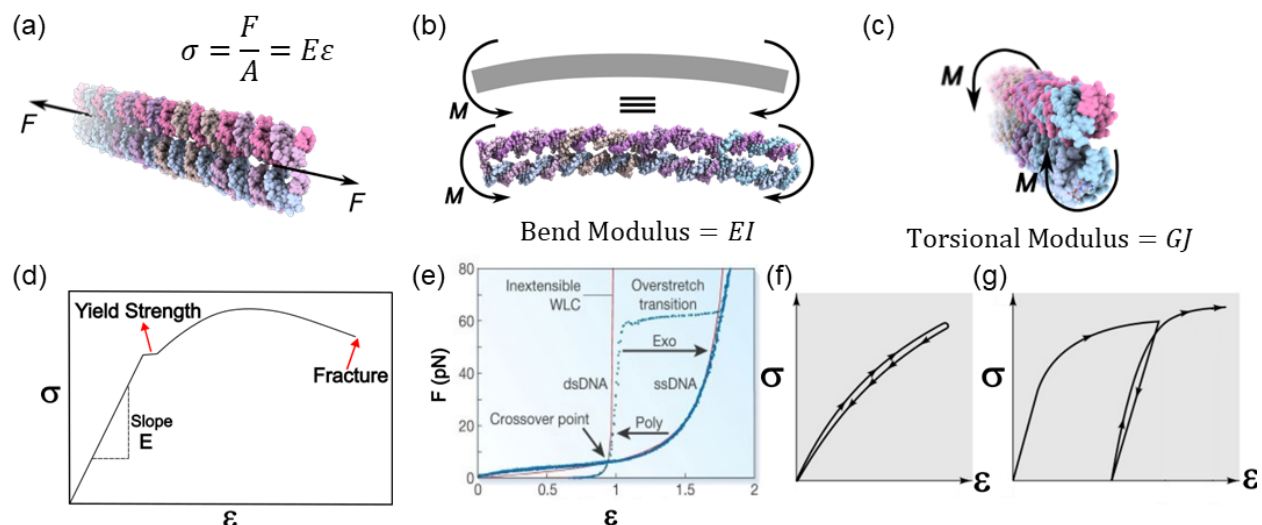


Figure 2. (a) A DNA beam under uniaxial loading, where σ is the stress, F represents the force, and A is the normal cross-sectional area. The stress σ is proportional to the strain ϵ (which is $\Delta L/L$ where L is length) with the constant E , the Young's Modulus. (b) The DNA beam under bending due to moments acting perpendicular to the axis, where M is the moment, and I is the area moment of inertia. (c) The beam under torsion where G is the shear modulus, and J is the polar moment of inertia. (d) The stress-strain curve of a general body with the slope representing the Young's modulus in the linear region. The turning point from linear to non-linear of the σ - ϵ plot marks the yield strength. As the general body extends more after yield, fracture will happen at the end. (e) The force vs. strain curves of dsDNA (left) and ssDNA (right), showing that their behaviors are characterized by distinct regimes with different Young's modulus.¹⁹⁰ The behaviors predicted by the inextensible worm-like chain model (WLC) for ssDNA and dsDNA are shown in red line for comparison. As the extension of dsDNA continues, the behavior transitions from pure dsDNA to ssDNA. The arrows indicate that it is possible to change the dsDNA behavior to ssDNA by exonuclease activity (Exo) and the other way around by polymerization (Poly), both at any constant force in the transition region (10-60 pN). (f)-(g) The force extension curves of a material under elastic (f) and plastic (g) loading.⁵⁸ (f) The loading and unloading curves of the elastic deformation are the same but in different direction. (g) With plastic deformation, only the elastic part of the deformation can be recovered during unloading. When loading again, there will be more permanent plastic deformation.

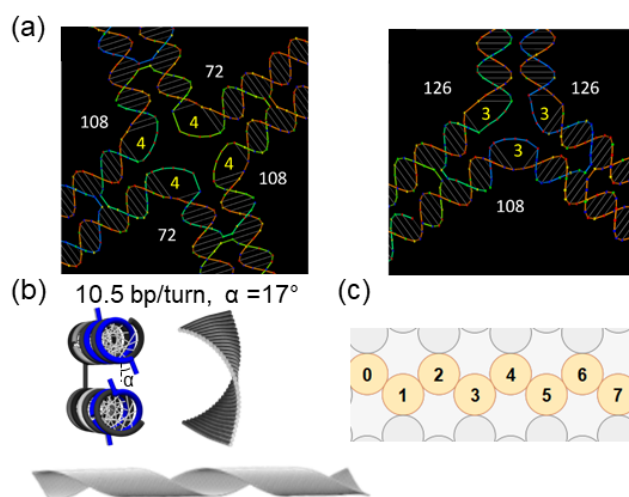


Figure 3. (a) Schematics of possible joint designs.⁶⁸ Left: 4-way junction. Right: 3-way junction. Integer full turns on dsDNA will place the joint to be on the same plane. Angles (white, in degree) are then controlled by the number of un-hybridized thymine (T) nucleotides on staples (yellow; e.g., 4-nt and 3-nt of ploy-T). (b) A DNA origami tile designed with a helical pitch of 10.67 bp/turn will experience strain due to the difference from the inherent 10.5 bp/turn of B-DNA.¹⁶ Neighboring helices will have a mismatch of $\sim 17^\circ$, which leads to a right-handed curvature as shown in the FEM computed structure on the right. This effect may be magnified if the tiles are polymerized into a long ribbon (shown in the bottom). (c) Cross-section of cadnano design in a honeycomb lattice. In this design, a planar structure would have a wave-like corrugated arrangement of the DNA bundles. Numbers indicate the dsDNA helices.

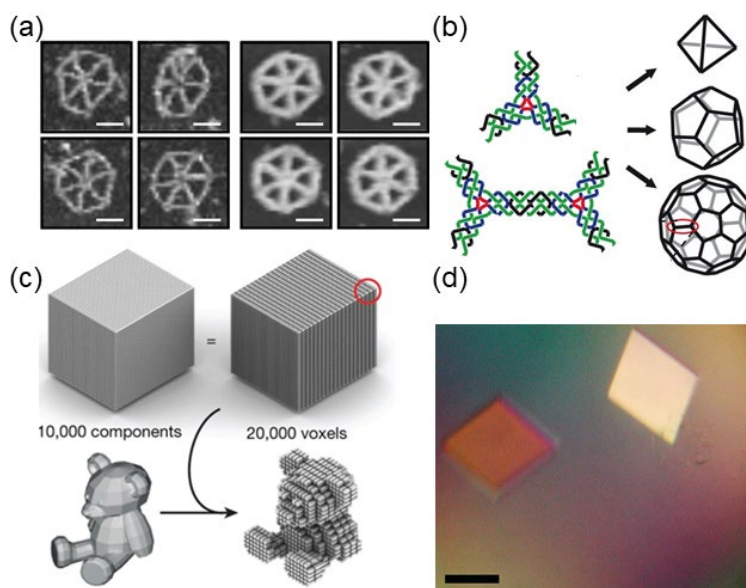


Figure 4. (a) TEM images of hexagon DNA origami with the same edge length but different cross-section.⁷⁸ The left four have 2 dsDNA bundles in each edge while the right four are composed of 6 dsDNA. Adding more dsDNA in an edge from 2 to 6 makes the edge more rigid and straight. Scale bar: 50 nm. (b) Symmetric motifs (*e.g.*, 3-point-star) from several oligonucleotides are assembled into tetrahedron, dodecahedron, and buckyball shapes.⁷⁹ (c) Schematics of DNA bricks approach. Like a machining process, this method conceptually starts with a cube and removes unneeded parts so that desired geometries such as a teddy bear will emerge from the annealing.⁸¹ (d) Optical image of macroscopic DNA crystals from tensegrity triangle motifs.⁸² Scale bar: 200 μm.

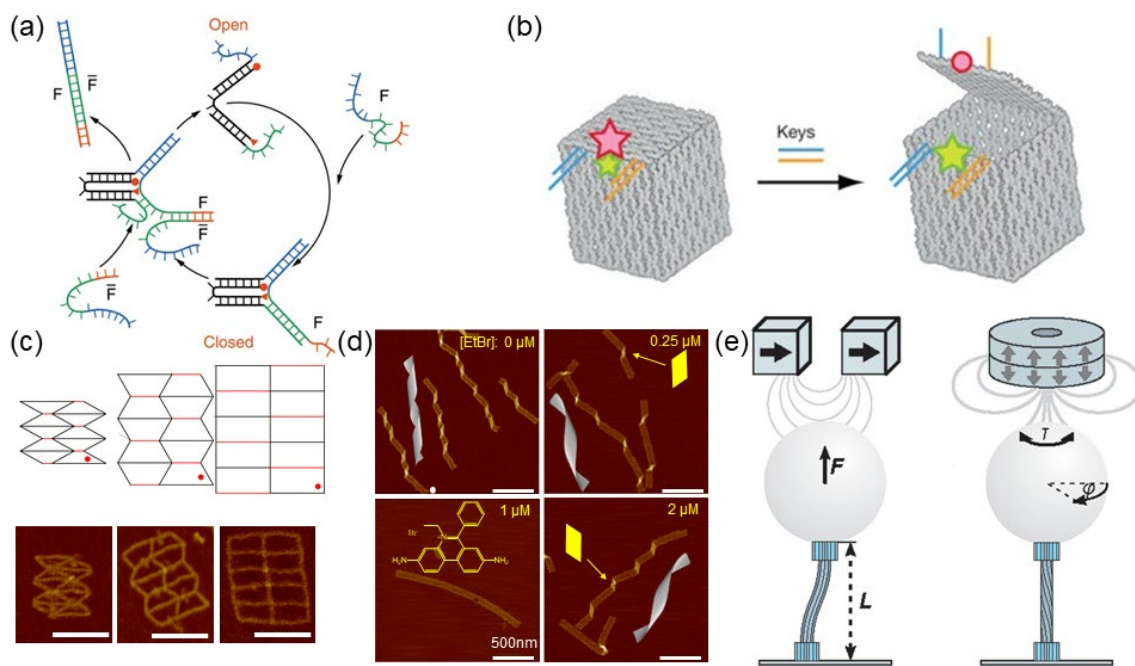


Figure 5. (a) A DNA tweezer that switches between open and closed states.⁸⁷ The structural changes are initiated by complementary strands F and \bar{F} that induce strand displacement. (b) A DNA box that can open and close its lid using a ssDNA hinge mechanism.¹¹² The box is locked initially by DNA strands (two independent groups, marked in blue and orange) and upon addition of keys the binding is released, thus opening the box with freedom of rotation from hinges. The Cy5 and Cy3 are depicted in red and green, respectively. Stars with different sizes represent emission with different intensities. Circle indicates a loss of emission. (c) Auxetic 2D DNA origami structures (re-entrant honeycomb) with jack edges (shown in red).⁹³ The jack edges can adjust its length with toehold-mediated strand displacement and addition of replacement strands. The structural deformations are performed by changing the length of jacks, demonstrating negative Poisson's ratios. The angle (noted by red dot) can vary from 30 to 60 to 90° (and *vice versa*). Scale bar: 100 nm. (d) Conformational control of polymerized DNA origami ribbons with chemical adducts.¹⁶ The increased concentration of intercalator ethidium bromide (EtBr) progressively changes the structures from right-handed to flat and then to left-handed conformations (noted by the yellow kink shape). Scale bar: 500 nm. (e) Schematics of magnetic tweezer experiments on DNA bundles with one end fixed on the surface and the other end attached to a magnetic bead.⁶³ The bead moves under magnetic fields, exerting external loadings on the DNA structure.

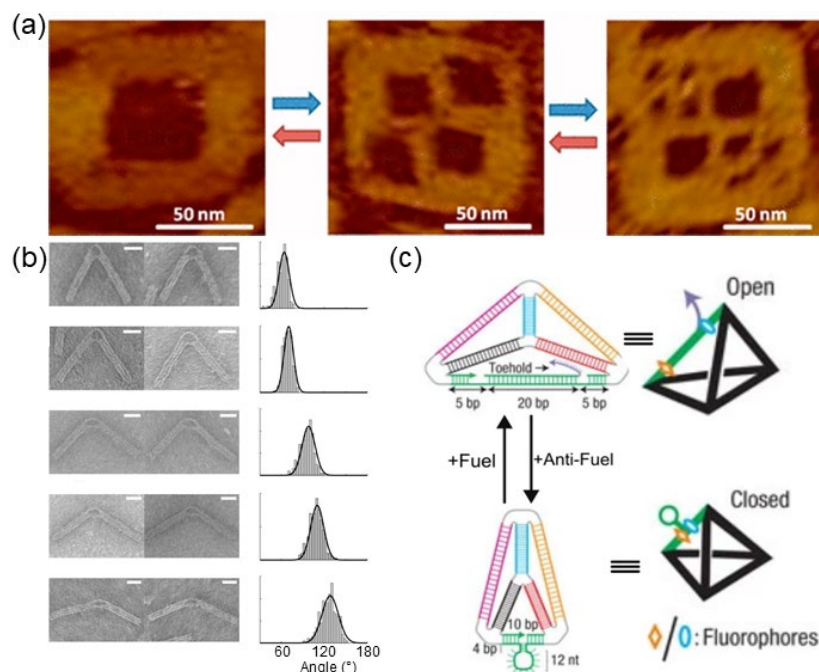


Figure 6. (a) AFM scans of a flat origami surface with 3 quasi-fractal patterns (left to right): 1, 4 and 10 cavities.¹³⁴ Scale bar: 50 nm. (b) TEM images of a DNA device with ssDNA hinge.¹⁴⁶ Different probability distributions are obtained for various lengths of ssDNA segments at the hinge. Scale bar: 20 nm. (c) Schematic design of reconfigurable DNA tetrahedron decorated with fluorophores, where Förster resonance energy transfer (FRET) between two fluorophores (orange rhombus and blue ellipse) is activated or deactivated upon structural changes via strand displacement.⁹⁶ The fuel strand binds with the single stranded free loop and extends the green edge, while the anti-fuel strand associates with the fuel strand (first, binding with the toehold to initiate strand displacement) and shrinks the green edge, leaving a free single stranded loop.

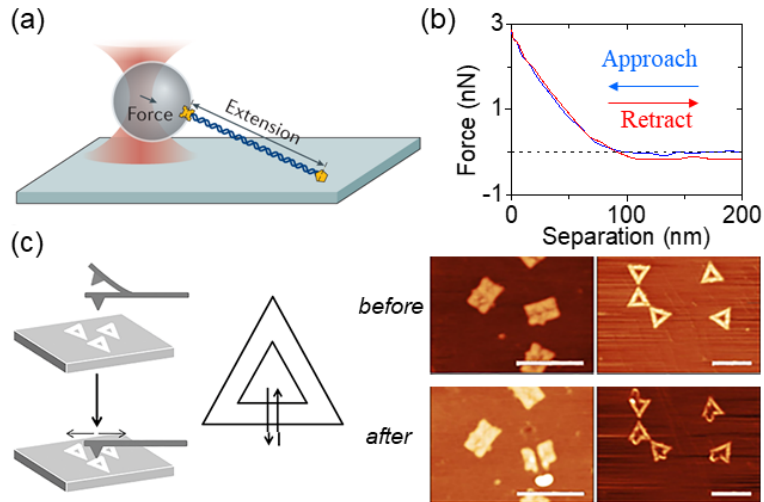


Figure 7. (a) Schematic illustration of a possible optical trap setting.¹⁹⁰ The DNA strand of interest can have one terminal attached to a surface while the other terminal is connected with an optical bead. The bead will be subjected under the optical trap. The laser beam exerts forces on the bead, pulling it away and thus stretching the DNA strand. (b) A pair of representative approach and retract force curves during the nanoindentation of an AFM tip on a single point of a macroscopic DNA crystal. The separation is the displacement from the lowest indented point. The indentation depth is approximately 100 nm.¹⁰⁸ (c) Manipulation of DNA origami using AFM through cutting.¹⁴³ Left: The schematics show the movement of the AFM tip. Right: AFM images present the comparison of two DNA origami samples (rectangle and triangle) before and after cutting. Scale bar: 200 nm.

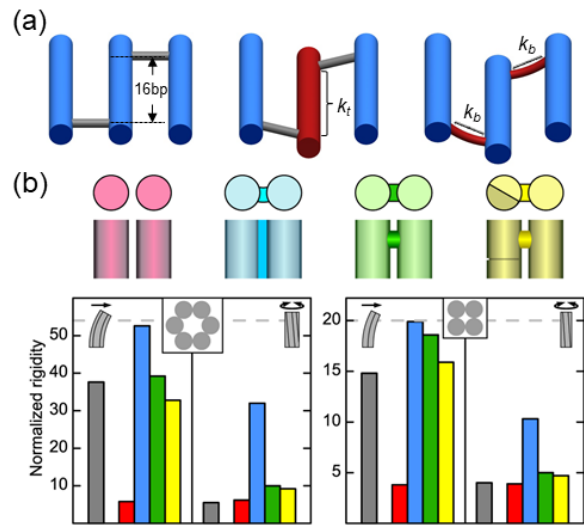


Figure 8. (a) Spring network system applied on a solid-piece origami tile, shown as a structural motif in a segment.⁵⁴ From left to right, the schematics show the undeformed motif (with blue and gray representing dsDNA rods and ssDNA crossovers, respectively), twisting of the double helix in the middle (maroon), and bending of crossovers (maroon). The length between neighboring crossovers is 16 bp. k_t is the torsional spring constant, while k_b is the bending spring constant of the crossovers. (b) Elastic beam theory models dsDNA bundles with different boundary conditions (red, fully disconnected; blue, fully attached; green, partially attached; and yellow, partially attached with discontinuity in the dsDNA bundles).⁶³ As a comparison, FEM simulations are shown in gray.

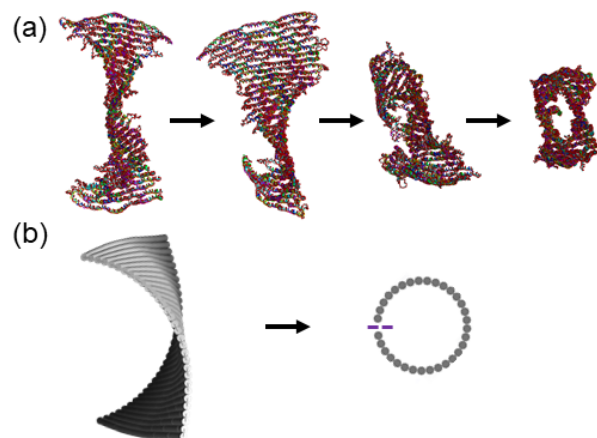


Figure 9. (a) Coarse-grained MD simulation on cyclization of a single-layer origami tile with initial curvature.¹⁶⁰ As the tile cyclizes, the initial curvature gradually disappears and the tile rolls from the boundary to the middle into a cylinder. The cylinder does not have a perfect circular cross-section. (b) Model for a spring system, where a perfect circular cross-section is assumed.¹⁶⁰

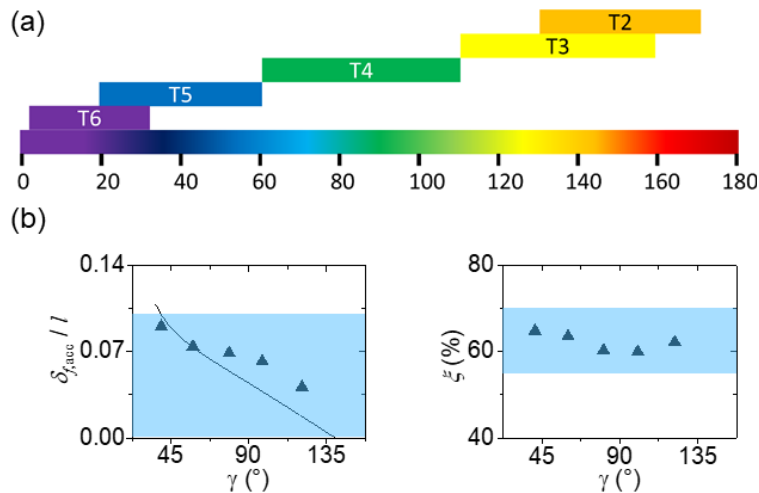


Figure 10. (a) Suggestions for unpaired ssDNA at the joints of a wireframe origami.⁶⁸ Un-hybridized thymine (T) nucleotides on staples are marked as T_n (e.g., T6 means 6-nt ploy-T, or TTTTTT). The length of ploy-T increases from 2 to 6 as the angle narrows from 180 to 0°. (b) Design guidelines for wireframe DNA origami that undergoes significant structural deformation (e.g., 10-50% relative changes).⁹³ Dimensionless flexure ($\delta_{f,acc}/l$) on the left and joint stretch (ξ) on the right as a function of angle γ which defines the conformation. The line is the prediction from the elasticity theory and the filled triangles denote the deformation data from coarse-grained MD simulations. $\delta_{f,acc}$ and l are the flexure and length of an edge in a wireframe DNA origami. Joint stretch ξ is defined as the length of a ssDNA segment at a joint divided by its fully stretched length. Blue shades indicate recommended regions for edge thickness and joint stretch. If the design recommendations are met, the wireframe structures will assume straight edges and sharp angles.

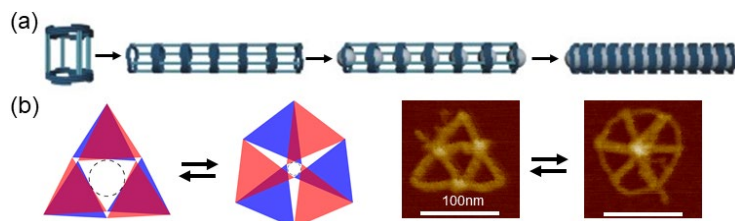


Figure 11. (a) A dynamic long and thin quadrangular prism or a cylindrical DNA template polymerized from monomers.¹¹¹ Left: a monomer with two rings and four pillars. Middle-left: polymerized cylindrical DNA template. Middle-right: the cylindrical DNA template with a liposome formed in the center of each ring. Right: liposomes merging together into a long single liposome by removing the pillars in the monomers. (b) 2D deployable Hoberman flight ring from DNA.¹⁷⁴ Left: schematics of the reconfiguration between open (triangle overall) and closed (hexagon overall) states. The inscribed circle is marked with a dotted line. The three red triangles are on top of the blue triangles. Note that the inside vertex of each red triangle is connected to that of the blue one on the opposite layer, thus forming a trefoil knot. Right: AFM images of open and closed states of the DNA origami. Scale bar: 100 nm.